Plant Cell Advance Publication. Published on October 17, 2018, doi:10.1105/tpc.18.00570

RESEARCH ARTICLE

An Effector from the Cyst Nematode *Heterodera schachtii* Derepresses Host rRNA Genes by Altering Histone Acetylation

Paramasivan Vijayapalani,[1] Tarek Hewezi,[1,a] Frederic Pontvianne,[2,3] and Thomas J. Baum[1*]
[1]Department of Plant Pathology and Microbiology, Iowa State University, Ames, IA 50011, USA
[2]CNRS, Laboratoire Génome et Développement des Plantes, UMR5096, F-66860, Perpignan, France
[3]Université de Perpignan Via Domitia, Laboratoire Génome et Développement des Plantes, UMR5096, F-66860, Perpignan, France

Short title: Nematode effector alters host plant histone acetylation

One-sentence summary: The 32E03 effector epigenetically regulates plant rRNA gene dosage, which is a crucial requirement to promote cyst nematode parasitism.

[a]Present Address: Department of Plant Sciences, University of Tennessee, Knoxville, TN 37996, USA
*To whom correspondence should be addressed: Tel: +1 515-294-5420; Email: tbaum@iastate.edu

The author responsible for distribution of materials integral to the findings presented in this article in accordance with the policy described in the Instructions for Authors (www.plantcell.org) is Thomas J. Baum (tbaum@iastate.edu)

ABSTRACT

Cyst nematodes are plant-pathogenic animals that secrete effector proteins into plant root cells to alter host gene expression and reprogram these cells to form specialized feeding sites, known as syncytia. The molecular mechanisms of these effectors are mostly unknown. We determined that the sugar beet cyst nematode (*Heterodera schachtii*) 32E03 effector protein strongly inhibits the activities of *Arabidopsis thaliana* histone deacetylases including the HDT1 enzyme, which has a known function in the regulation of rRNA gene expression through chromatin modifications. We determined that plants expressing the 32E03 coding sequence exhibited increased acetylation of histone H3 along the ribosomal DNA (rDNA) chromatin. At low 32E03 expression levels, these chromatin changes triggered the derepression of a subset of ribosomal RNA (rRNA) genes, which were conducive to *H. schachtii* parasitism. By contrast, high levels of 32E03 caused profound bidirectional transcription along the rDNA, which triggered rDNA-specific small RNA production leading to RNA-directed DNA methylation and silencing of rDNA, which inhibited nematode development. Our data show that the 32E03 effector alters plant rRNA gene expression by modulating rDNA chromatin in a dose-dependent manner. Thus, the 32E03 effector epigenetically regulates plant gene expression to promote cyst nematode parasitism.

INTRODUCTION

Plant-pathogen interactions are complex and dynamic and involve diverse recognition and signal transduction networks. At the heart of these interactions, massive gene expression changes govern the outcome. The mechanisms initiating and regulating gene expression are of particular interest in understanding plant-pathogen interactions. The manipulation of host chromatin is a powerful strategy to alter gene expression, but the mechanistic understanding of plant chromatin changes during plant-pathogen interactions, particularly how pathogens regulate host chromatin changes, remains largely obscure. The full relevance of this mechanism in plant-pathogen interactions is still emerging (Alvarez et al., 2010; Berr et al., 2012; Dowen et al., 2012; Yu et al., 2013; Ding and Wang, 2015; Rambani et al., 2015; Yang et al., 2015; Zhu et al., 2016).

Pathogens deliver a repertoire of effectors into plant cells that counteract defense responses or alter host cells to modulate cellular processes to support pathogen survival. Cyst nematodes are plant-parasitic animals that reprogram plant root cells by secreting effectors to create a large, highly metabolically active nutrient sink known as the syncytium, from which they feed (Hewezi and Baum, 2013; Mitchum et al., 2013; Hewezi et al., 2015). Obviously, effectors are of particular interest when exploring pathogen-triggered gene expression changes in the host.

Here we present the function of the 32E03 effector of the sugar beet cyst nematode *Heterodera schachtii*, which also infects the model plant *Arabidopsis thaliana*. *H. schachtii* effector 32E03 is a homolog of the uncharacterized soybean cyst nematode (*Heterodera glycines*) 32E03 effector (GenBank Accession number AF500036) (Gao et al., 2003). Our analyses unveil that the 32E03 effector interacts with the *A. thaliana* FK506-binding protein FKBP53 and the plant-specific tuin-type histone deacetylase (HDAC) HDT1 in the plant nucleolus. FKBP53 is an immunophilin-type peptidyl propyl cis-trans isomerase and a histone chaperone (Li and Luan, 2010). Tuin-type HDACs play roles in plant growth and responses to environmental stimuli (Colville et al., 2011; Luo et al., 2012; Yano et al., 2013; Zhao et al., 2015; Han et al., 2016). Guided by this discovery, we show that the 32E03 protein acts as a potent inhibitor of plant histone deacetylase activities. Because we had identified HDT1 and FKBP53 as 32E03 interaction partners, we functionally characterized 32E03 deploying the reported HDT1/FKBP53 effects on rDNA regulation as an example of how HDAC inhibition by a pathogen effector can alter host gene expression. In these studies, we determined that the 32E03 effector mediates a dose-dependent epigenetic control of

plant rRNA gene expression, which regulates rRNA gene dosage and influences cyst nematode parasitism.

RESULTS AND DISCUSSION

Effector 32E03 is Important for *H. schachtii* Pathogenicity

We determined by *in situ* hybridization that *32E03* mRNA accumulates in the dorsal esophageal gland cell of *H. schachtii* (Figure 1A), which is a hallmark characteristic of many nematode effectors. Furthermore, we confirmed the presence of *32E03* mRNA in pre-parasitic and parasitic developmental stages of *H. schachtii* by RT-qPCR analyses (Figure 1B). In order to determine the biological relevance of 32E03 in cyst nematode-*A. thaliana* interactions, we tested the pathogenicity of *H. schachtii* nematodes in which *32E03* gene expression was strongly reduced by RNA interference (RNAi). After confirming the downregulation of *32E03* mRNA in the RNAi nematodes by RT-qPCR analyses (Figure 1C), RNAi and control nematodes (incubated in *yellow fluorescent protein* (*YFP*) double-stranded RNA (dsRNA) or only buffer) were used separately to inoculate wild type *A. thaliana* plants. RNAi nematodes produced fewer adult female nematodes compared to control nematodes (Figure 1D), revealing reduced pathogenicity. The infection assay data, thus, confirmed that 32E03 is a crucial effector in cyst nematode parasitism.

In addition to depriving infective nematodes of this effector function by RNAi, we also expressed the *32E03* coding sequence without the secretory signal peptide sequence (Figure 2A) under control of the *35S* promoter in *A. thaliana* (*32E03* line) to assess effector function. It can be expected and has been shown repeatedly that *in planta* expression of an effector will profoundly alter plant morphology and will either increase or decrease plant susceptibility (Hewezi et al., 2008; Hewezi et al., 2010; Hewezi et al., 2015). While screening for non-segregating homozygous 32E03-expressing transgenic lines in the T3 generation, we determined that a portion of these lines showed strong morphological phenotypes (small leaves, short roots and an overall stunted growth), while other lines showed no noticeable phenotype and resembled the wild type *A. thaliana* plants (Figure 2B). This observation suggested a dose effect of the 32E03 transgene *in planta*. When these two types of transgenic lines were assayed for *32E03* mRNA and protein expression, we found high *32E03* mRNA and protein expression in the transgenic lines that displayed distinct morphological phenotypes, whereas the transgenic lines without visible phenotype changes showed relatively lower expression of *32E03* (Figure 2C and D). We chose at least three

homozygous lines each from these two groups for further study and designated transgenic *A. thaliana* lines showing high or low expression of *32E03* as *32E03-H* or *32E03-L*, respectively. We assessed susceptibility to *H. schachtii* of the two types of transgenic lines. Interestingly, we observed a severe reduction in the susceptibility of *32E03-H* lines, while *32E03-L* lines were more susceptible when compared to wild type *A. thaliana* plants (Figure 2E). These results imply that relatively low 32E03 expression levels are conducive to parasitism. By contrast, high 32E03 expression levels are detrimental to the plant and the nematode. Furthermore, these data show that 32E03 has a powerful function *in planta* and that the mode of action of this effector influences the plant-nematode interaction.

In order to discern that the lower susceptibility of the *32E03-H* line is not just due to the smaller root size of these lines but due to an actual change in plant-nematode interactions, we measured the size of syncytia developed at later stages in the requisite *A. thaliana* lines. We found a significant reduction in average size of syncytia found in the *32E03-H* line (56,116 μm^2) when compared to those found in the *32E03-L* line (145,145 μm^2) and the wild type plants (138,308 μm^2). While root size likely plays a role in the reduced number of females developing on the *32E03-H* line (we determined that fewer nematodes penetrated into the *32E03-H* line roots than into wild type plant roots; Figure 2F), there also are significant syncytial changes taking place as a function of high 32E03 levels that lead to smaller syncytia and likely to lower numbers of developing females.

Effector 32E03 Interacts and Co-localizes with *A. thaliana* Histone Deacetylase HDT1 and Histone Chaperone FKBP53

While the 32E03 effector has no detectable amino acid sequence similarity to other proteins in GenBank, using the PSORT algorithm (Nakai and Horton, 1999), 32E03 was predicted to contain a bipartite nuclear localization signal (NLS; Figure 2A), which suggested that 32E03 likely becomes a plant nuclear protein once delivered into plant cells by the nematode, as has been shown for other nematode effectors (Elling et al., 2007; Hewezi et al., 2015; Zhang et al., 2015). This was confirmed by the transport of GFP-GUS-tagged 32E03 into plant nuclei (Figure 3A).

Identification of host plant proteins that physically interact with nematode effectors is a promising approach to elucidate effector function (Hewezi et al., 2008; Hewezi et al., 2010; Hewezi et al., 2015; Pogorelko et al., 2016). To this end, we performed yeast two-hybrid (Y2H)

screens using the *32E03* coding sequence without the secretory signal peptide sequence as bait for prey libraries derived from *H. schachtii*-infected *A. thaliana* root cDNA (Hewezi et al., 2008). We identified *A. thaliana* tuin-type histone deacetylase HDT1 (AT3G44750.1) and FK506-binding protein FKBP53 (AT4G25340.1) as *bona fide* interactors of 32E03 (Figure 3B).

A. thaliana HDT1 is a tuin-type (plant-specific) HDAC that deacetylates histone H3 at lysine 9 (H3K9), which in turn leads to dimethylation of H3K9 (Lawrence et al., 2004). Interestingly, both *A. thaliana* HDT1 and FKBP53 function as transcriptional repressors of ribosomal RNA (rRNA) genes (Lawrence et al., 2004; Li and Luan, 2010). The finding that both 32E03-interacting proteins have documented functions in the same pathway gives credence to the physiological relevance of the discovered protein interactions and raises the possibility that 32E03 may function in regulating rRNA gene expressions in *A. thaliana* during nematode infection.

As an additional approach to scrutinize these protein interactions, we used co-immunoprecipitation (co-IP) assays. For this purpose, nuclear extracts of a *32E03*-expressing *A. thaliana* line and the wild type were subjected to pull-down assays using anti-32E03 antibodies, and the interacting proteins were detected by protein gel blotting. HDT1 and FKBP53 were immunodetected only in the immunoprecipitates of the *32E03* line and not of the wild type *A. thaliana* control plants (Figure 3C), confirming the strong and stable association of 32E03 with the plant HDT1 and FKBP53 proteins.

We further tested the relevance of our Y2H data by gene expression analyses for the two interacting proteins. If the interactions of 32E03 with HDT1 and FKBP53 are of relevance *in vivo*, the two 32E03 interactors would have to be expressed in nematode-infected roots at the site of infection. To test this, we analyzed the expression of *HDT1* and *FKBP53* genes in *H. schachtii*-infected *A. thaliana* roots by RT-qPCR and found significant upregulation of both genes in the infected roots when compared to uninfected roots (Supplemental Figure 1). Furthermore, we determined the activity of the *HDT1* and *FKBP53* promoters in *A. thaliana* transgenic lines (*HDT1pro:GUS* and *FKBP53pro:GUS*) using the GUS reporter gene. Following *H. schachtii* infection, the developing syncytia in both transgenic lines showed strong GUS expression (Figure 3D), indicating strong promoter activity of *HDT1* and *FKBP53* in the same root cells into which the nematode is delivering the 32E03 effector, thus, fulfilling a critical requirement for an actual interaction of 32E03 with HDT1 and FKBP53 *in vivo*.

Finally, we used immunolocalization analysis to confirm our Y2H interaction results. In mammalian cells, HDACs function in concert with nuclear FKBP proteins in regulating gene expressions (Yang et al., 2001), and one can postulate that similar functions may also be conserved in plants. In support, Y2H assays performed by us show the interaction between *Arabidopsis* HDT1 and FKBP53 (Figure 4). Thus, we hypothesized that 32E03 may alter the gene regulation activity of HDT1 and FKBP53, in particular their known regulatory activity on rRNA genes. To test this, we conducted immunolocalization analyses using confocal microscopy to detect 32E03 and HDT1 or FKBP53 in nuclei of a *32E03* line. We detected co-localization foci of 32E03 with HDT1 or FKBP53 in these nuclei. While co-localization of 32E03 and HDT1 was predominant in the nucleolus (Figure 3E), 32E03 co-localization with FKBP53 was evident in the nucleolus as well as in the nucleoplasm (Figure 3E). These results confirm that the effector co-localizes with HDT1 and FKBP53 in the nucleolus, which again confirms our Y2H results, but maybe more importantly, is in line with a function of 32E03 in altering rRNA gene expression in *A. thaliana*. Collectively, our Y2H, co-IP, promoter analyses, and immunolocalization data indicate that the 32E03 effector establishes strong and stable interaction and co-localization with HDT1 and FKBP53 *in planta*, and these interactions likely have a physiological relevance in plant-nematode interactions.

32E03 is a potent inhibitor of *A. thaliana* HDACs

The fact that we could demonstrate *bona fide* interaction of the nematode effector 32E03 with the plant histone deacetylase HDT1, obviously begged the question if this effector can alter HDAC activity. We explored this question in a series of experiments. First, we measured total HDAC activities in nuclear extracts from 7 day-old whole wild type and *32E03* expression seedlings. In the extracts from *32E03-H* and *32E03-L* lines, HDAC activity was significantly reduced when compared to wild type plants (Figure 5A), and the reduction in enzyme activity was more pronounced in the *32E03-H* line, suggesting that 32E03 is the cause of inhibition of total HDAC activity. To confirm this, we measured HDAC activity in wild type plant nuclear extract as a function of added purified recombinant 32E03 protein. In the presence of 32E03, HDAC activity was significantly inhibited when compared to enzyme activity in the absence of 32E03 (Figure 5B). The level of HDAC inhibitory action of 32E03 in the wild type plant nuclear extract was comparable to that of the potent HDAC inhibitor trichostatin, which was added to a set of wild-

type plant nuclear extract (Figure 5B). Our results convincingly show that 32E03 inhibits HDAC activity *in planta* to a degree comparable to that of the HDAC inhibitor trichostatin.

We then determined if our HDAC activity assay in fact measures HDT1 activity by comparing HDAC activity between nuclear extracts of an HDT1 over-expression line (*HDT1* expression was driven by the *35S* promoter; Supplemental Figure 2) and wild type plants. In the *HDT1* over-expression line, HDAC activity was significantly increased relative to the wild type (Figure 5B), which documented that HDT1 activity was indeed measured as a part of total HDAC activity in our assays. Interestingly, we determined in subsequent experiments that the HDAC activity measured in the nuclear extracts of wild type plants and the 32E03 expression line is largely due to HDAC enzymes other than HDT1 because HDAC activity in the extracts of a *HDT1* knockdown mutant *(hdt1*) was not different from that of wild type plants (Figure 5B). In other words, while we showed upregulation of the *HDT1* promoter in the syncytium, *HDT1* expression in whole-plants appears relatively low.

In order to determine if 32E03 also inhibits HDT1, we needed to employ an indirect approach because we were not aware of a specific HDT1 activity assay *in planta*. For this purpose, we measured HDAC activity in nuclear extracts of the *HDT1* over-expression line as a function of added purified recombinant 32E03 protein at two concentrations. Both 32E03 preparations inhibited the elevated HDAC activity in the nuclear extracts of the *HDT1* over-expression line and the higher 32E03 concentration had an almost complete HDAC inhibitory effect comparable to that of trichostatin (Figure 5B). These data showed that the 32E03 effector is a powerful and promiscuous inhibitor of HDAC activities including that of HDT1.

Because of this wide inhibition of HDACs by 32E03, we performed additional targeted Y2H assays in order to explore which other HDAC enzymes might interact with 32E03. Given the large size of the HDAC gene family, we only assayed the tuin-type HDACs HDT2 (AT5G22650.1), HDT3 (AT5G03740.1), and HDT4 (AT2G27840.1) as the closest HDT1 relatives. In addition, we included the RPD3-type HDAC HDA6 (AT5G63110.1), because, similar to HDT1, it has known functions in rRNA gene regulation (Earley et al., 2010). Interestingly, none of these proteins interacted with 32E03 in the YTH assays (Figure 6). While strong Y2H interaction is a promising indicator that the proteins in question truly interact, the absence of protein interaction in Y2H assays does not preclude possible protein interactions *in vivo*. Because a more detailed analysis of HDAC interactions with 32E03 is beyond the scope of this paper, we did not further explore which

specific HDACs are inhibited by 32E03 at this point. However, we took this analysis one step further by conducting genetic analyses of the *hdt1* and *hda6* mutants. Even though, we could not show 32E03 interaction with HDA6, we included the *hda6* mutant because of the documented role of HDA6 in rRNA gene regulation (Earley et al., 2010). As one could expect from the broad HDAC inhibitory function of 32E03, the *hdt1* and *hda6* mutant lines showed no morphological or nematode susceptibility phenotypes when compared to the wild type (Figure 7), suggesting robust functional redundancy among HDACs in *A. thaliana*. We also assayed if mRNA expression of *HDT1* or *HDA6* is altered in the *32E03-H* and *32E03-L* lines and determined that the steady-state mRNA abundance of these genes is not altered by expression of the effector (Figure 8).

Our data convincingly show broad HDAC activity inhibition by 32E03. Furthermore, we showed 32E03 interaction with and inhibition of HDT1, a HDAC that has been shown to regulate rRNA gene expression through chromatin modifications. These conclusions directed our attention to the regulation of rRNA genes as a function of 32E03.

Expression of 32E03 Mediates rDNA Chromatin Modifications and Alters 45S Pre-rRNA Abundance

As mentioned above, HDT1 has been shown to deacetylate H3K9 along rDNA chromatin, which subsequently leads to dimethylation of H3K9 and repression of rDNA expression (Lawrence et al., 2004; Pontes et al., 2007; Li and Luan, 2010). Our finding of inhibition of HDAC activities by 32E03 in *A. thaliana* plants naturally begged the question if the presence of this effector in plant cells would modulate the acetylation and methylation status of H3K9 along the rDNA chromatin and would alter rRNA gene expression. In *A. thaliana*, rRNA genes are tandemly arrayed head-to-tail at chromosomal loci known as nucleolus organizer regions (NORs), and the *A. thaliana* genome has two such NORs. Each rRNA gene is separated from adjacent genes by an intergenic spacer (IGS). RNA polymerase I (Pol I) transcribes 45S pre-rRNA primary transcripts, which are processed into catalytic rRNAs (18S, 5.8 S and 25S) by sequential cleavage of the external and internal transcribed spacers (ETS and ITS) in the nucleolus. To further delineate the function of 32E03, levels of H3K9Ac and H3K9me2 along the rDNA chromatin stretches as shown in Figure 9A were compared between *32E03-L* and *-H* lines and wild type *A. thaliana* plants by chromatin immunoprecipitation (ChIP)-qPCR assays. Confirming the HDAC inhibitory function of 32E03, we found elevated levels of H3K9Ac throughout the coding and noncoding regions of

rDNA in the *32E03-H* and *32E03-L* lines as compared to wild type *A. thaliana* plants (Figure 9B), while H3K9me2 levels were substantially reduced in the same locations (Figure 9B). In both the *32E03-H* and *32E03-L* lines, the H3K9 modifications assayed were unaltered at *ACTIN 2* and *AtSN1* retrotransposon loci when compared to wild type *A. thaliana* plants (Figure 9B). In other words, these ChIP-qPCR data indicate that the 32E03 effector modulates histone modifications along the rDNA chromatin in *A. thaliana* plants.

The above discoveries lead us to hypothesize that 32E03-mediated H3K9 hyperacetylation along the rDNA chromatin would open rDNA chromatin, thereby allowing an increased transcription of rRNA genes. To test this, we quantified 45S pre-rRNA transcripts in *32E03-L* and *-H* lines by RT-qPCR. While we indeed confirmed the expected high abundance of 45S pre-rRNA transcripts in the *32E03-L* line, we surprisingly observed a significant reduction in 45S pre-rRNA transcripts in the *32E03-H* line (Figure 9C). This result raised the distinct possibility that the difference in 45S pre-rRNA abundance in *32E03-L* and *32E03-H* may be the cause for the earlier described variation in their morphology and susceptibility phenotypes. If this were true, then increased 45S-pre-rRNA abundance would be beneficial to nematode infection, while a severe reduction in pre-rRNA abundance would be detrimental. To validate this conclusion, we compared the levels of 45S pre-rRNA transcripts in *A. thaliana* root segments containing *H. schachtii*-induced syncytia and neighboring root segments without syncytia. We found a significant increase in 45S pre-rRNA abundance (7.4 fold) in root segments containing syncytia when compared to the root segments without syncytia (Figure 9D). These data demonstrate that *H. schachtii* infection indeed upregulates the rRNA gene expressions in or around the syncytial feeding cells.

High Levels of 32E03 in *A. thaliana* Trigger RNA-directed DNA Methylation of rDNA

It remained unclear why the *32E03-H* line in spite of increased acetylation of H3K9 along the rDNA chromatin exhibited a strong repression of the rRNA genes. We hypothesized that the repression of rRNA genes in the *32E03-H* line is a plant response to out-of-control transcription events triggered by high concentrations of 32E03. To test this hypothesis, we used ChIP-qPCR analyses to evaluate if the 32E03-mediated uncontrolled 'open' structure of rDNA chromatin in the *32E03-H* line is accompanied by increased RNA polymerase II (Pol II) occupancy. Significantly elevated Pol II-mediated transcription along the rDNA would be expected for serendipitous transcription triggered by an opened chromatin state rather than the normal core-

promoter-triggered Pol I-mediated transcription of rRNA genes. We documented an approximately 7-23-fold increased Pol II occupancy in the rDNA coding and non-coding regions in the *32E03-H* line as compared to wild type *A. thaliana* plants (Figure 10A). Importantly, occupancy of Pol II at IGS regions in the *32E03-H* line was increased to 19-fold when compared to wild type plants. In contrast and as expected, Pol II occupancy was not elevated in the *32E03-L* line when compared to wild type *A. thaliana* plants (Supplemental Figure 3A). Pol II ChIP signals at *ACTIN 2* and *AtSN1* transposons did not vary between the two *32E03* transgenic lines and wild-type plants (Figure 10A and Supplemental Figure 3A), indicating the likely enhanced transcription activity of Pol II along the rDNA chromatin in the *32E03-H* line. We then assessed IGS-derived transcript levels in *32E03-H* plants by random-primed and strand-specific RT-PCR assays in selected IGS regions (Figure 10B). As could be expected from the elevated Pol II occupancy along the IGS in the *32E03-H* line, we documented enhanced sense as well as anti-sense IGS transcripts in the *32E03-H* line when compared to wild type plants (Figure 10C), which is indicative of profound bidirectional transcription along the IGS regions in the *32E03-H* line. In contrast, bidirectional transcription along the IGS was not elevated in the *A. thaliana 32E03-L* line (Supplemental Figure 3B). These findings are consistent with an enhanced derepression of cryptic Pol II transcription units along the rDNA in the *32E03-H* line, which is likely the result of a 32E03-mediated uncontrolled 'opened' state of the rDNA chromatin. Having discovered the enhanced bidirectional transcription along IGS regions in the *32E03-H* line, prompted us to postulate that bidirectional transcription would result in the production of dsRNA, which could trigger biogenesis of small RNAs (sRNAs) in the *32E03-H* line. Therefore, we analyzed the accumulation of IGS-derived sRNAs in the *32E03-H* line by RNA gel blot analysis. Using probes corresponding to the IGS regions (Figure 10B), we detected an increase in accumulation of 21- and 24-nt sRNAs in the tested *32E03-H* line relative to wild type *A. thaliana* plants (Figure 10D). The presence of these sRNAs in the *32E03-H* line pointed towards the possibility that RNA-directed *de novo* DNA methylation (RdDM) could be responsible for the observed repression of rRNA genes in the *32E03-H* line. A similar phenotype has been described in an *A. thaliana hda6* knock-out mutant, in which cryptic RNA pol II transcriptional activity was accompanied by an over accumulation of small RNAs that directed *de novo* DNA methylation and gene silencing (Earley et al., 2010).

In *A. thaliana*, stable gene silencing is mediated by DNA methylation (Zilberman et al., 2007; Lister et al., 2008; Becker et al., 2011; Schmitz et al., 2011). While cytosine methylation in CG

and CHG contexts is maintained by methyltransferase MET1 and plant-specific CMT3 methyltransferase, respectively (Lindroth et al., 2001; Kankel et al., 2003), maintenance of asymmetric CHH methylation relies on the RdDM pathway (Matzke, 2016). To test our hypothesis that silencing of rRNA genes in the *32E03-H* line is the regulatory mechanism postulated above, we compared the cytosine methylation levels at the core rDNA promoter region (Figure 10E) of the *32E03-H* line with that of wild type *A. thaliana* plants. Bisulphite sequence analyses revealed an approximately three-fold hypermethylation of the rDNA promoter in the CHH context in the *32E03-H* line when compared to wild type *A. thaliana* plants (Figure 10F and G), which indicates that high levels of 32E03 in *A. thaliana* plants triggered the RdDM pathway. Interestingly, we discovered that methylation in the CG and CHG contexts also were elevated, which suggests that high 32E03 levels triggered additional regulatory mechanism that resulted in the hypermethylation of the rDNA promoter region. These major quantitative changes in cytosine methylation are consistent with the observed reduction in 45S pre-rRNA abundance in the *32E03-H* line. Therefore, presence of 32E03 at high levels as found in the *32E03-H* line, led to silencing of rRNA genes, which significantly interfered with cyst nematode parasitism. In a wider sense, the 32E03 effector-triggered hypermethylation of rDNA renders plant cells unable to sustain normal syncytium function and therefore causes decreased parasitism. In contrast to the hypermethylation of the rDNA promoter found in the *A. thaliana 32E03-H* line, cytosine methylation of the rDNA promoter did not vary between the *32E03-L* line and wild type plants (Supplemental Figure 3C).

Low Levels of 32E03 in *A. thaliana* Derepress a Subset of VAR1 rRNA Genes

Our findings that the *32E03-L* line showed an increase in 45S pre-rRNA abundance and an overall phenotype conducive to *H. schachtii* parasitism, suggested that 32E03 is a positive regulator (i.e., a derepressor) of rRNA genes and, thus, of *H. schachtii* parasitism. We set out to obtain molecular proof to test this hypothesis. The specific nature of rDNA variants in *A. thaliana* provided an opportunity to further dissect the mechanism of 32E03 function *in planta*. In *A. thaliana* ecotype Col-0, there are at least four rRNA gene variants (*VAR1-4*), based on sequence variation within the repetitive region in the 3' ETS (Pontvianne et al., 2010). These four rRNA variants are expressed in newly germinated seeds, but by 10-14 days after germination and throughout the remaining vegetative development, the majority of *VAR1*, accounting for ~50% of the total rRNA gene pool, is selectively silenced by an epigenetic mechanism (Pontvianne et al., 2012; Pontvianne

et al., 2013). The rRNA gene dosage is controlled according to the cellular demand for ribosomes and protein synthesis. The silenced rRNA gene subtypes were mapped to the *NOR* on chromosome 2, while the active rRNA gene subtypes are mapped to the *NOR* on chromosome 4 (Chandrasekhara et al., 2016). Therefore, it is a tempting hypothesis that the 32E03 effector function leading to an increase in 45S pre-rRNA transcription in the *32E03-L* line is due to a derepression of rRNA genes that are normally silenced in growing plants.

To test this hypothesis, we took advantage of the single nucleotide polymorphisms (SNPs) naturally existing within the ETS and ITS of *A. thaliana* VAR1, VAR2 and VAR3 rRNA variants, which create unique restriction endonuclease recognition sites (Chandrasekhara et al., 2016). We adapted cleaved amplified polymorphic sequence (CAPS) assays to analyze expression of rRNA subtypes VAR1 (6645), VAR2 (4302) and VAR3 (7122) in the *32E03-L* line and wild type *A. thaliana* plants. For this, root cDNA was PCR-amplified, digested with VAR1-6645*,* VAR2-4302 or VAR3-7122 SNP-specific restriction enzyme and analyzed by agarose gel electrophoresis. Among the rRNA subtypes analyzed, VAR1-6645C was detected only in the *32E03-L* line and not in wild type *A. thaliana* plants (Figure 11A), which indicated derepression of the VAR1-6645C rRNA subtype as a function of the 32E03 effector.

To determine if this derepression also can be found in the *H. schachtii*-induced syncytium, rRNA subtypes were analyzed in wild-type *A. thaliana* root segments containing *H. schachtii*-induced syncytia and in neighboring root segments without syncytia. Interestingly, VAR1-6645C was detected only in root segments containing syncytia and not in segments without syncytia (Figure 11B). Thus, these CAPS data confirmed that the derepression of rRNA subtype VAR1-6645C occurs in *A. thaliana* root cells into which the nematode had delivered the 32E03 effector during the infection process. Though derepression of a single rRNA subtype by the 32E03 effector is documented here, the possibility of derepression of multiple rRNA subtypes by 32E03 cannot be ruled out. We further elaborated on this phenomenon by comparing the proportion of VAR1 in rRNA pools of the *A. thaliana 32E03-L line* and wild type plants. For this purpose, we determined the ratio of VAR1 to 45S pre-rRNA (VAR1:45S) by RT-qPCR analyses. In the *A. thaliana 32E03-L* line, we found a remarkable increase in the VAR1:45S ratio relative to wild type plants at both time points analyzed (Figure 11C). In addition, analysis of the VAR1:45S ratio in wild type *A. thaliana* root segments containing *H. schachtii*-induced syncytia revealed an increase in the VAR1:45S rRNA to 3.5-fold when compared to root segments without syncytia (Figure 11D).

Collectively, the CAPS and VAR1:45S ratio data further confirm the function of 32E03 effector in the derepression of rRNA genes in host plant cells.

In summary, our data document that 32E03 is a potent cyst nematode effector that the parasite deploys to inhibit the function of *A. thaliana* HDACs (including HDT1) to mediate rDNA chromatin modifications with the outcome of a derepression of rRNA genes. This regulation of plant genes by the 32E03 effector not only provides key insights into plant-parasite interactions, but also reveals the apparent requirement of fine-tuning of rRNA gene dosage in the nematode induced syncytium. In addition, there likely are additional, so far unknown consequences of 32E03-mediated inhibition of HDACs. Certain HDACs have been documented to play roles in modulating defense gene expressions and the manifestation of plant resistance (Zhou et al., 2005; Kim et al., 2008; Choi et al., 2012; Ding et al., 2012). Furthermore, tuin-type HDACs have been shown to act as negative regulators of elicitor-induced plant cell death (Bourque et al., 2011; Dahan et al., 2011). Interestingly, the HC toxin produced by the plant-pathogenic fungus *Cochliobolus carbonum* (Brosch et al., 1995; Ransom and Walton, 1997; Sindhu et al., 2008) and the Depudecin toxin of the fungus *Alternaria brassicicola* (Wight et al., 2009) inhibit plant HDACs to suppress defense responses and to enable the necrotrophic life style of these fungi within their hosts. Here, we report a very different, and so far, unique molecular mechanism of how a parasite deploys an effector to modulate a plant-specific HDAC (and likely a histone chaperone although not further studied in this report) to fine-tune host rRNA dosage to sustain the demands and rigors of nematode parasitism. Taken one step further, it is highly interesting, yet not surprising, that plants have evolved a unique mechanism that is triggered by effector-mediated chromatin modulation, and it remains to be seen if such mechanisms are also triggered by other phytopathogens.

In this cyst nematode pathosystem, it is evident that the nematode parasite is 'walking a tight rope' by having to increase rRNA abundance without triggering the host plant's gene silencing through DNA hypermethylation. Although a variety of epigenetic mechanisms in plants are associated with pathogen interactions, in particular bacterial and fungal pathogen infections (Ding and Wang, 2015; Zhu et al., 2016), direct evidence for how pathogen effectors may manipulate epigenetic regulation in the host remains very limited. The TrAP protein of two plant Geminiviruses inhibits H3K9 methylation in *A. thaliana* to counter host defense (Castillo-Gonzalez et al., 2015). Recently, it has been shown that an effector of the oomycete pathogen *Phytophthora sojae* acts as a modulator interfering with the function of the plant histone

acetyltransferase GCN5 complex and suppresses defense genes at an epigenetic level (Kong et al., 2017). The RomA effector of the human bacterial pathogen *Legionella pneumophila* acts as a histone methyltransferase to directly methylate host histones, which represses immune gene expression (Rolando et al., 2013). Finally, an effector of the animal parasite *Toxoplasma* manipulates the function of a host histone deacetylase complex, which is linked to blocking of immune gene expression (Olias et al., 2016). The 32E03 effector function documented here reveals a powerful mechanism for how a parasite alters plant chromatin structure to achieve gene expression changes required for infection success.

METHODS

Plant Material

Arabidopsis thaliana plants were grown under sterile conditions on Murashige and Skoog (MS) medium containing vitamins (Plant Media) and 2% sucrose at 26°C or in soil at 23°C in a growth chamber under long-day (16 h-light/8 h-dark photoperiod with fluorescent bulbs generating soft white light). For stable plant expression, the *32E03* coding sequence was PCR-amplified from *Heterodera schachtii* cDNA, while the *HDT1* coding sequence was amplified from *A. thaliana* cDNA. Amplified products were individually cloned into the binary vector pBI121. *A. thaliana* (ecotype Col-0 for *32E03* or C24 for *HDT1*) was transformed by the floral-dip method (Clough and Bent, 1998). Transformants were screened on Murashige and Skoog medium containing 50 mg/L kanamycin, and homozygous lines were identified in the T3 generation. *A. thaliana hdt1* (CS348580) and *hda6* (Murfett et al., 2001) mutant seeds were obtained from the Arabidopsis Biological Resource Center.

Nematode Infection Assay

Ten-day-old *A. thaliana* seedlings grown on modified Knop's medium (Sijmons et al., 1991) at 24°C under 16 h-light/8 h-dark were inoculated with J2 *H. schachtii* nematodes (Baum et al., 2000). Four weeks post inoculation, adult females in each plant were counted, and the data were analyzed by a modified *t*-test using the Statistical Software Package SAS ($P<0.05$). Root segments containing *H. schachtii*-induced syncytia and adjacent root segments without syncytia were dissected under a light microscope as described in (Hermsmeier et al., 2000).

Nematode Penetration Assay

Penetration of *H. schachtii* into roots of *A. thaliana* seedlings was determined 4 days post inoculation (Hewezi et al., 2008). The number of penetrating nematodes in each root system was counted under bright-field illumination using a Zeiss Axiovert 100 microscope. Each plant line was replicated 16 times, and three independent experiments were conducted. Average numbers of penetrating nematodes were calculated, and statistically significant differences were determined in a modified *t*-test using the statistical software package *SAS* ($P<0.05$).

Syncytial Measurements

Size of syncytia was measured 21 days post inoculation of *A. thaliana* with *H. schachtii* (Hewezi et al., 2008). For each line, 20 single-female syncytia were randomly selected, size was measured and average size for each line was determined. Statistically significant differences were determined in a modified *t*-test using the statistical software package *SAS* ($P < 0.05$).

RNA Extraction and cDNA Synthesis

H. schachtii eggs, pre-parasitic J2 juveniles from a hatch chamber, parasitic J2, J3, J4 and adult females from nematode-infected *Brassica oleracea* were collected and frozen. Total RNA was extracted from nematode and plant tissues using the Versagene RNA Tissue Kit (Gentra Systems) or RNeasy Plant Mini Kit (Qiagen). After treating the RNA with RNase-free DNase I (Invitrogen), cDNA was synthesized using the qScript cDNA SuperMix (Quanta Biosciences).

***In Situ* Hybridization**

Parasitic *H. schachtii* J3 nematodes were isolated from infected *A. thaliana* plants as described (Gao et al., 2001), and *32E03* mRNA was detected by *in situ* hybridization (de Boer et al., 1998) with a gene-specific digoxigenin (DIG)-labeled (Boehringer, Mannheim) antisense- or sense-cDNA probe synthesized by asymmetric PCR (de Boer et al., 1998). Hybridization signals were detected using anti-DIG antibodies conjugated to alkaline phosphatase (ALP) (diluted 1:100) and 5-bromo-4-chloro-3-indolyl-phosphate with nitro blue tetrazolium as substrate in a Zeiss Axiovert 100 inverted compound light microscope.

RNAi of *32E03* in *H. Schachtii*

32E03 expression in pre-parasitic *H. schachtii* J2s was down-regulated by the double-stranded RNA (dsRNA) soaking method (Sukno et al., 2007). Two non-overlapping coding regions (5': 1-200 bp and 3': 286-486 bp) of the *32E03* coding sequence without the secretory signal peptide sequence were PCR-amplified from *H. schachtii* cDNA. A *Yellow fluorescent protein* (*YFP*) gene sequence (1-195 bp) was amplified from p35S-SPYNE (provided by Jorg Kudla, Universitty of Munster). The PCR products were used as templates to synthesize dsRNA transcripts *in vitro* using the MEGAscript RNAi kit (Ambion). Freshly hatched nematodes were soaked in M9 buffer (43 mM Na_2HPO_4, 22 mM KH_2P0_4, 2 mM NaCl and 4.6 mM NH_4Cl) containing dsRNA (3.5 mg/ml), 50 mM octopamine (Sigma-Aldrich), 1 mM spermidine (Sigma-Aldrich) and 0.05% gelatin in a moisture chamber at 28°C for 24 h.

Yeast Two-Hybrid Screening and Protein Interaction Assays

The *32E03* coding sequence without the secretory signal peptide was PCR-amplified from *H. schachtii* cDNA with an artificial start codon and fused in-frame to the *GAL4* DNA binding domain in plasmid pGBKT7 (Clontech). The resultant bait construct was designated as pTH22. cDNA of *H. schachtii*-infected *A. thaliana* roots was cloned into plasmid pGADT7 (Clontech) to construct prey libraries (Hewezi et al., 2008). Yeast AH109 strain harboring the prey library and Y187 strain harboring the bait construct were mated and screened on a double dropout medium (SD/-Leu/-Trp; DDO) and subsequently on a high stringency quadruple dropout medium (SD/-Leu/-Trp/-Ade/-His; QDO) containing X-α-Gal (5-bromo-4-chloro-3-indolyl α-D-galactopyranoside) using the BD Matchmaker Library Screening kit (Clontech). From yeast cells that displayed a positive protein interaction, prey plasmids were rescued in *E. coli* and sequenced. For protein interaction assays, *A. thaliana HDT1* was cloned into pGBKT7, while *A. thaliana HDT2*, *HDT3, HDT4, HDA6* and *FKBP53* were cloned into pGADT7. A prey vector harboring the human *Lamin C* gene (Clontech) served as control. DNA and protein sequences were analyzed with the BLAST alogrithms (http://blast.ncbi.nlm.nih.gov/blast/.cgi).

***HDT1* and *FKBP53* Promoter Assay**

Promoter constructs of *HDT1* and *FKBP53* were generated by ligating 1006 and 970 bp DNA fragments upstream of *A. thaliana HDT1* or *FKBP53* coding regions, respectively, into the pBI101 binary vector to drive expression of a *β-glucuronidase* (*GUS*) reporter gene. Wild type *A. thaliana*

plants were transformed with either of the binary constructs. Stable homozygous transgenic lines were infected with *H. schachtii* and GUS expression was analyzed by histochemical staining (Jefferson et al., 1987) in a Zeiss SV-11 microscope. Images were captured using a Zeiss AxioCam MRc5 digital camera and processed using Zeiss Axiovision software (version 4.8).

Protein Synthesis *In Planta*

For subcellular localization analyses, the PCR-amplified *32E03* coding sequence without the secretory signal peptide coding sequence was cloned between the *35S* promoter and the *GFP-GUS* fusion reporter gene in a modified pRJG23 vector (Grebenok et al., 1997). The construct was delivered into onion epidermal cells by particle bombardment, and the bombarded samples were incubated at 25°C in the dark for 16 hrs. Fluorescence signals were analyzed with a Zeiss Axiovert 100 microscope.

Protein Synthesis in *Escherichia coli* and Purification

The *32E03* coding sequence without the secretory signal peptide was PCR-amplified from *H. schachtii* cDNA with a start codon, a 6X histidine tag at the 3' end and a stop codon and cloned into plasmid pET28a (Novagen). *E. coli* strain C41 (DE3) (Lucigen) was transformed with this construct. Transformants were grown at 37°C in Luria Bertoni medium (supplemental with 100 µg/ml ampicillin) to A_{600} 0.5 and induced with 0.6 mM isopropyl-D-thiogalactopyranoside for 3 h. Cells were harvested, resuspended in phosphate buffered saline (PBS: 0.05 M phosphate, pH 7.4, 0.25 M NaCl, 2 mM phenylmethanesulfonyl fluoride and protease inhibitor cocktail tablets (Roche)), sonicated and centrifuged at 10,000 g. The lysate was applied onto cobalt resin (Pierce Biotechnology) and washed with PBS containing increasing concentrations of imidazole (35, 50 or 60 mM). Resin-bound 32E03 recombinant protein was eluted with 500 mM imidazole, dialyzed in PBS, and purity of the protein was verified in a Novex 8-16% Tris-glycine SDS-PAGE (Life Technologies). Polyclonal antibodies against recombinant 32E03 were generated in mouse at the Iowa State University Hybridoma Facility.

Co-IP and Immunodetection

For co-immunoprecipitation assays, nuclei were isolated from *A. thaliana* plants and lysed as described (Wierzbicki et al., 2008). Nuclear lysate was immunoprecipitated with mouse anti-

32E03 antibodies overnight at 4°C. For immunodetection of proteins in *A. thaliana* plants, total protein was extracted in extraction buffer (10 mM Tris-HCl, pH 7.4, 300 mM NaCl, 5 mM EDTA, 1 mM PMSF and 1 mM DTT). The immunoprecipitate or total protein was separated in Novex 4-16% Tris-glycine SDS-PAGE (Life Technologies) and electroblotted onto a polyvinylidenediflouride membrane (PVDF) (Bio-Rad). The blot was probed with anti-32E03 antibodies (dilution 1:2000), rabbit anti-HDT1 polyclonal antibodies (provided by Craig Pikaard, Indiana University) (dilution 1:1000) rabbit anti-FKBP53 polyclonal antibodies (developed to oligopeptide representing FKBP53 amino acids 350-363 by Genscript) (dilution 1:1000) or mouse anti-ACTIN monoclonal antibodies (ABclonal) (1:1000). The total protein blot was developed with goat anti-mouse antibodies conjugated to horseradish peroxidase (HRP) (Genscript) (dilution 1:10,000) and detected using the LumiSensor Chemiluminescent HRP Substrate kit (GenScript). The immunoprecipitate sample blot was developed using anti-mouse or anti-rabbit antibodies conjugated to HRP and detected using the SuperSignal Western Femto Maximum Sensitivity Substrate (Thermo Scientific).

Immunostaining

Nuclei of *A. thaliana* plants were isolated and immunostained as described (Durut et al., 2014) . A combination of anti-32E03 antibodies and anti-HDT1 antibodies or anti-FKBP53 antibodies at a dilution of 1:100 in PBS was applied onto a slide pre-coated with nuclei and incubated overnight at 4°C. The nuclei were labeled with anti-rabbit-Alexa Fluor 488 and anti-mouse-Alexa Fluor 594 antibodies (Abcam) at a dilution of 1:1000, counterstained with DAPI (4', 6-diamidino-2-phenylindole), mounted using the Vectashield medium (Vector Laboratories), and analyzed in a Leica SP5 X inverted confocal microscope. The images were processed using the Leica Application Suite 2.3.0. All images are projections of optical sections.

Histone Deacetylase Assay

Nuclear extract of *A. thaliana* plants (7-d-old) was prepared using the Epiquick Nuclear Extraction Kit I (Epigentek), and total histone deacetylase activity in nuclear extracts was measured in the presence or absence of recombinant 32E03 (500 or 1500 nM) or trichostatin (500 nM) using the Epigenase HDAC Activity/Inhibition Direct Assay Kit (Epigentek). Protein concentration in the nuclear extract was determined using the Coomassie Protein Assay Reagent (Thermo Scientific).

ChIP-qPCR

Nuclei of *A. thaliana* seedlings were isolated, and chromatin was immunoprecipitated using anti-H3AceK9 antibodies (Thermo Scientific), anti-H3me2K9 antibodies (Abcam) or anti-RNA polymerase II antibodies (Santa Cruz Biotechnology, Inc.) as described (Wierzbicki et al., 2008). Abundances of rDNA regions, *SN1* and *ACTIN 2* in ChIP samples relative to input were determined by qPCR.

Random and Strand-Specific RT-PCR and qPCR

For random RT-PCR and strand-specific RT-PCR, total RNA of *A. thaliana* roots was treated with DNase I, and using random or strand-specific primers and the RevertAid First Strand cDNA synthesis kit (Thermo Scientific), first-strand cDNA was synthesized. The first-strand cDNA was PCR-amplified using the amplicon-specific primers and analyzed by agarose gel (1.5%) electrophoresis followed by SYBR Safe staining. Images of the strand-specific RT-PCR products were analyzed using the *ImageJ* software (https://imagej.nih.gov/ij/). For qPCR, ten-fold diluted cDNA or genomic DNA, 10 pmol primer and iQ SYBR Green Supermix (BioRad) were used for amplification in an iCycler IQ system (Bio-Rad Laboratories). Data were analyzed using the comparative CT method (Livak and Schmittgen, 2001). Gene expression in *A. thaliana* plants and nematodes were normalized to *ACTIN* gene expression. qPCR conditions were as follows: 95°C for 3 min, followed by 40 cycles of each of 10 sec at 95°C, 30 sec at 60°C. A dissociation curve was produced at the end of the cycling phase to ensure that a single PCR product was produced with no primer dimers.

rRNA Variant SNP Analysis

rRNA variants in 12 day-old *A. thaliana* plants were analyzed as described (Chandrasekhara et al., 2016). cDNA of *A. thaliana* roots or root segments enriched in *H. schachtii* syncytia was used to amplify rRNA variants by PCR. The products were gel eluted, digested with *Sph*I (VAR1-6645), *Alu*I (VAR2-4302) or *Msp*I (VAR3-7122) and resolved in 2.5 % agarose gels followed by SYBR Safe staining.

Small RNA Gel Blot Hybridization

598 Small RNAs of *A. thaliana* seedlings were isolated using the Nucleospin miRNA kit (Machery
599 Nagel), resolved in a 15% TBE-urea gel (Life Technologies) and blotted onto a nylon membrane
600 (GenScreen Plus). Oligonucleotide probes corresponding to regions indicated in Figure 10B were
601 synthesized using the mirVana probe construction kit (Ambion), purified with the Performa DTR
602 Gel Filtration Cartridge (EdgeBio), hybridized to small RNAs on the blots at 42°C overnight, and
603 recognized using anti-DIG-ALP antibodies (Roche) at RT for 45 min. The blot was processed
604 using the DIG Wash and Block Buffer Set reagents (Roche) and hybridization signal was detected
605 using the CDP-Star Chemiluminescence Reagent (Perkin Elmer).
606
607 **DNA Methylation Analysis**
608 Genomic DNA of *A. thaliana* seedlings was extracted using the DNA Easy Plant Mini kit (Qiagen),
609 and 500 ng of DNA was digested with *BamHI* prior to bisulphite conversion using the Epitect
610 Bisulphite kit (Qiagen). The rDNA promoter sequence was PCR-amplified, cloned in the pGEM-
611 T Easy vector (Promega), and the clones were analyzed using the CyMATE method (Hetzl et al.,
612 2007).
613 Sequences of all the primers used in this study are listed in Supplemental Table 1.
614
615 **Accession Numbers**
616 TAIR accession numbers of *A. thaliana* genes are: AT3G44750 (*HDT1*), AT5G22650 (*HDT2*),
617 AT5G03740 (*HDT3*), AT2G27840 (*HDT4*), AT5G63110 (*HDA6*), AT4G25340 (*FKBP53*) and
618 AT1G49240 (*ACTIN 8*). GenBank accession number of *H. schachtii β-ACTIN* is AY443352 and
619 *Heterodera glycines 32E03* is AF500036.
620
621 **Supplemental Data**
622 **Supplemental Figure 1.** Expression of *HDT1* and *FKBP53* in *H. schachtii* infected *A. thaliana*
623 wild type plants.
624 (Supports **Figure 3.**)
625 **Supplemental Figure 2.** Expression of *HDT1* in *A. thaliana HDT1* and *hdt1* lines.
626 (Supports **Figure 5.**)
627 **Supplemental Figure 3.** Cytosine methylation of rDNA promoters does not vary between *A.*
628 *thaliana 32E03-L* line and wild type plants.

(Supports **Figure 11.**)

Supplemental Table 1. Sequence of primers.

ACKNOWLEDGEMENTS

This work was supported by Hatch Act and State of Iowa funds and by grants to T.J.B. from the Iowa Soybean Association, the North Central Soybean Research Project, and the United States Department of Agriculture NIFA-AFRI (Grant No. 2015-67013-23511). F.P. was supported by the French Laboratory of Excellence project TULIP (ANR-10-LABX-41; ANR-11-IDEX-0002-02). We thank Craig S. Pikaard, Indiana University for providing polyclonal antibodies to *A. thaliana* HDT1. We thank Jorg Kudla, University of Munster for sharing the p35S-SPYNE vector. We thank Tom Maier, Iowa State University for technical assistance.

AUTHOR CONTRIBUTIONS

P.V. conceived, designed and performed the Y2H interaction, co-localization, co-IP, RNAi experiments and all the experiments related to functional characterization of 32E03. T.H. isolated the effector, designed and conducted localization, Y2H screening and GUS assays, and generated yeast prey libraries and transgenic lines. F.P. performed cytosine methylation data analyses and participated in designing the co-localization and rRNA experiments. T.J.B. supervised and guided the project. P.V. and T.J.B. wrote the manuscript with input from all authors. All authors reviewed and commented on the manuscript.

Figure legends:

Figure 1 *H. schachtii* effector *32E03* has important pathogenicity function.

(A) *32E03* mRNA is abundantly expressed in the dorsal esophageal gland (DG) of *H. schachtii*. *In situ* hybridization of digoxigenin-labeled *32E03* antisense- or sense-cDNA probes to *32E03* transcripts expressed in the DG of third-stage (J3) nematodes. S, stylet; Scale bar = 10 µm.
(B) *32E03* mRNA is detectable throughout the life cycle of *H. schachtii*. Total RNA was extracted from eggs, second-stage (J2), third-stage (J3), fourth-stage (J4) and adult female nematodes. cDNA was synthesized, and abundance of *32E03* mRNA was quantified by qPCR in each life stage in three technical replicates. *β-ACTIN* mRNA abundance was used to normalize *32E03* expression. The fold values indicate values relative to that of eggs ± SE.
(C-D) RNAi of *32E03* expression in *H. schachtii* inhibits pathogenicity. (C) Downregulation of *32E03* expression in RNAi *H. schachtii*. Pools of newly hatched *H. schachtii* J2 nematodes were soaked in *32E03* double-stranded RNA (dsRNA), *yellow fluorescent protein* (YFP) dsRNA or only buffer. Total RNA of nematode pools was extracted, cDNA was synthesized and abundance of *32E03* was quantified by qPCR. *β-ACTIN* mRNA abundance was used to normalize *32E03* expression. Expression values are shown as fold changes relative to nematodes soaked in buffer. The experiment was repeated three times, each with three technical replicates. Similar results were obtained from three independent experiments and only data from one representative experiment are shown. Shown data are means ± SE. 5' or 3' indicates 5' or 3' region of the *32E03* mRNA, respectively. Mean values significantly different from that of nematodes soaked in buffer were determined by unadjusted paired *t*-test and are indicated by an asterisk (P<0.1%).
(D) Downregulation of *32E03* expression in *H. schachtii* inhibits pathogenicity. *A. thaliana* wild type plants were inoculated with RNAi nematodes or nematodes soaked in buffer, and 4 weeks after inoculation, the number of adult females per plant was determined. Data are the average number of adult females ± SE (n = 30). The experiment was repeated at least three times. Similar results were obtained from three independent experiments. Data from one representative experiment are shown. Mean values significantly

different from that of the nematode soaked in buffer were determined by unadjusted paired *t*-tests ($P < 0.05$) using the *SAS* statistical software package and are indicated by an asterisk.

Figure 2 Expression of 32E03 in *A. thaliana* alters morphology and susceptibility to *H. schachtii*.

(A) Amino acid sequence of 32E03 effector of *H. schachtii*. N-terminus of 32E03 contains a secretory signal peptide (in bold). Bipartite nuclear localization signal predicted by PSORT algorithm is underlined.
(B) Morphology of transgenic *A. thaliana* plants expressing 32E03. *A. thaliana* wild type plants were transformed with a construct containing the *32E03* coding sequence without the secretory signal peptide under control of the *35S* promoter. In the T3 generation, two types of homozygous lines (*32E03-H* and *32E03-L*) varying in morphology were identified. Root length is the average measurement of 20 plant roots ± SE.
(C) Quantification of *32E03* mRNA in transgenic *A. thaliana* lines. Total RNA of *A. thaliana 32E03-H* and *32E03-L* lines was extracted and the levels of *32E03* mRNA were quantified by qPCR. *ACTIN 2* was amplified as reference. Data are the mean ± SE. The experiment consisted of three independent biological replicates, each encompassing three technical replicates.
(D) Quantification of 32E03 protein in transgenic *A. thaliana* lines. Total protein of *A. thaliana 32E03-H* and *32E03-L* lines was resolved in Novex 4-16% Tris-glycine SDS-PAGE, electroblotted onto a PVDF membrane, probed with anti-32E03 antibodies and detected using LumiSensor Chemiluminescent HRP Substrate. RUBISCO was detected as loading control.
(E) Expression of 32E03 in *A. thaliana* plant affects susceptibility to *H. schachtii*. Five independent *A. thaliana 32E03-H* and *32E03-L* lines each were inoculated with *H. schachtii* J2 nematodes, and four weeks after inoculation, the number of adult females per plant were counted. *H. schachtii*-inoculated *A. thaliana* wild type plant was used as control. Each experiment was repeated three times. Data are the average of adult females per plant in each plant type ± SE (n = 30). Mean values significantly different from that of wild-type plants were determined by unadjusted paired *t*-tests ($P < 0.05$) using the *SAS* statistical software package and are indicated by an asterisk.
(F) Root penetration by *H. schachtii* juveniles is reduced in *A. thaliana 32E03-H* line. *A. thaliana 32E03-H* and *32E03-L* lines were inoculated with *H. schachtii* J2 nematodes, and four days of post inoculation, the number of nematodes that had penetrated into each plant-type was counted. *H. schachtii* inoculated wild type plants were used as control. The experiment comprised three independent *32E03-H* and *32E03-L* lines each. Data are the average number of penetrated nematodes in each plant type ± SE (n = 16). Mean values significantly different from that of wild-type plants were determined by unadjusted paired *t*-tests ($P < 0.05$) using the *SAS* statistical software package and are indicated by an asterisk.

Figure 3 32E03 expressed in *A. thaliana* interacts and co-localizes with HDT1 and FKBP53 proteins.

(A) 32E03 accumulates in the plant nucleus. A plasmid containing the *32E03* coding sequence without the secretory signal peptide fused to the *GFP-GUS* gene was delivered into onion epidermal cells using biolistic bombardment, and the bombarded cells were analyzed by epifluorescence microscopy. Bar = 100 µm.
(B) 32E03 interacts with *A. thaliana* HDT1 and FKBP53 in yeast. Yeast cells co-transformed with the *32E03* bait plasmid and the *HDT1* or *FKBP53* prey plasmid were grown on a low stringency double dropout (DDO) medium and a high stringency quadruple dropout (QDO) medium in the presence of X-α Gal to confirm protein interaction. Empty prey vector or prey vector containing human *Lamin C* served as controls.
(C) 32E03 synthesized in *A. thaliana* forms a complex with endogenous HDT1 and FKBP53. Nuclear extract of a 32E03-expressing *A. thaliana* line was immunoprecipitated with anti-32E03 antibodies, and the immunoprecipitates (IP) were analyzed by protein gel blot using anti-32E03, anti-HDT1 or anti-FKBP53 antibodies. HDT1, FKBP53 and ACTIN 2 in input nuclear extract was detected as loading control.
(D) *H. schachtii* infection upregulates *A. thaliana HDT1* and *FKBP53* promoter activities. *A. thaliana* transgenic plants harboring the *GUS* gene under the control of the *HDT1* (*HDT1pro:GUS*) or *FKBP53* (*FKBP53pro:GUS*) promoter were inoculated with *H. schachtii*, and the infected roots were analyzed for

GUS expression by histochemical assays. dpi, days post inoculation. N, nematode; S, syncytium; P, lateral root primordium. Scale bar = 10 µm.
(E) 32E03 co-localizes with endogenous *A. thaliana* HDT1 and FKBP53. Nuclei of 32E03-expressing *A. thaliana* line were immunostained with anti-32E03 antibodies in combination with anti-HDT1 or anti-FKBP53 antibodies, probed with secondary antibodies conjugated to Alexa Fluor 488 or Alexa Fluor 594 and counterstained with 4', 6-diamidino-2-phenylindole (DAPI). About 200 nuclei in each preparation were analyzed by confocal microscopy. no, nucleolus; np, nucleoplasm. Scale bar = 5 mm.

Figure 4 *A. thaliana* HDT1 and FKBP53 interact.
Yeast cells co-transformed with the *HDT1* bait plasmid and the *FKBP53* prey plasmid were grown on a low stringency double dropout (DDO) medium and a high stringency quadruple dropout (QDO) medium in the presence of X-α Gal to confirm protein interaction. Empty prey vector or prey vector containing human *Lamin C* served as controls.

Figure 5 32E03 inhibits histone deacetylase (HDAC) activities.

(A) Expression of 32E03 in *A. thaliana* inhibits HDAC activities. HDAC activities of the *32E03-H* and *32E03-L* lines were compared to that of the wild type plants.
(B) Recombinant 32E03 inhibits HDAC activities. HDAC activities in the wild type, *HDT1* and *hdt1* plants were measured in the presence or absence of recombinant 32E03 protein (r32E03; 500 or 1500[a] nM) or trichostatin (TSA, 500 nM).
In A and B, plants of the tested genotypes were grown in a randomized block design. For each biological replicate, plants were sampled randomly to prepare pools for each line. Nuclei of *A. thaliana* pools were isolated and nuclear extracts were prepared for HDAC assays. The experiment comprised three biological replicates, each with three technical replicates. Data are the mean values ± SE. Statistically significant changes in HDAC activity were determined by unadjusted paired *t*-test and are indicated by an asterisk (P≤0.1).

Figure 6 32E03 does not interact with other tuin-type histone deacetylases or HDA6 of *A. thaliana* in Y2H system.

Yeast cells co-transformed with the *32E03* bait plasmid and the *HDT2, HDT3, HDT4* or *HDA6* prey plasmid were grown on a low stringency double dropout (DDO) medium and a high stringency quadruple dropout (QDO) medium in the presence of X-α Gal to confirm protein interaction. Empty prey vector or prey vector containing human *Lamin C* served as controls.

Figure 7 Susceptibility to *H. schachtii* is not altered in *A. thaliana hdt1* and *hda6* lines.

Three independent lines of *A. thaliana hdt1* and *hda6* each were inoculated with *H. schachtii* J2 nematodes, and four weeks after inoculation, the number of adult females per plant were counted. *H. schachtii*-inoculated *A. thaliana* wild type plants were used as control. The experiment was repeated three times. Similar results were obtained in three independent experiments. Data of one representative experiment are shown. Data are the average of adult females per plant in each plant-type ± SE (n = 30). Mean values significantly different from that of wild-type plants were determined by unadjusted paired *t*-tests (P < 0.05) using the *SAS* statistical software package.

Figure 8 Expression of *HDT1* and *HDA6* is unaltered in A*. thaliana 32E03-H* and *32E03-L* lines.

Root total RNA of *A. thaliana* wild type plants and the *32E03-H* and *32E03-L* lines was extracted, cDNA was synthesized and *HDT1* and *HDA6* expression was quantified by qPCR. Wild type plants were used as control. *ACTIN 2* was amplified as reference. Tested genotypes were grown in randomized block

designs. For each biological replicate, plants were sampled randomly to prepare pools for each genotype. The experiment consisted of three biological replicates, each encompassing three technical replicates. Data are the mean ± SE. Statistically significant difference in the mean values was analyzed by unadjusted paired *t*-test (P=0.05).

Figure 9 Expression of the *32E03* coding sequence in *A. thaliana* mediates rDNA chromatin modifications and alters 45S pre-rRNA abundance.

(A) Diagram showing *A. thaliana* rDNA regions. The indicated regions were amplified in qPCR assays shown in Figure 9B, 10A and Supplemental Figure 3A. *25S* and *18S*, coding region; +1, transcription start site.
(B) 32E03 expression in *A. thaliana* causes histone H3 modifications along the rDNA. Chromatin of *32E03-H* and *32E03-L* lines was immunoprecipitated with anti-H3K9Ac or anti-H3K9me2 antibodies and subjected to qPCR to quantify the rDNA regions indicated in A. Wild type plants were used as control. *ACTIN 2* and *SN1* were amplified as reference. Pro, promoter.
(C) Abundance of 45S pre-rRNA in *A. thaliana 32E03-H* and *32E03-L* lines. Total RNA of roots of *A. thaliana* wild type plants and *32E03-H* and *32E03-L* lines was extracted. Wild-type plants were used as control. 45S pre-rRNA in the 32E03 expression lines was determined relative to wild-type plants.
(D) Abundance of 45S pre-rRNA in *A. thaliana* wild-type root segments enriched in *H. schachtii*-induced syncytia. Wild type plants were inoculated with *H. schachtii* J2s. Root segments enriched in *H. schachtii*-induced syncytia (root+syncytium) and adjacent root segments without syncytia (root-syncytia; control) were dissected at 10 days post inoculation.
For B, C and D, plants of the tested genotypes/treatments were grown in randomized block designs. For each biological replicate, plants were sampled randomly to prepare pools for each genotype/treatment. Experiments comprised three biological replicates, each with three technical replicates. Similar results were obtained from three independent experiments. Data from one representative experiment each are shown in B, C, and D. Data are the means ± SE.
For C and D, root cDNA was synthesized and 45S pre-rRNA was quantified by qPCR. *Arabidopsis ACTIN 8* was amplified as reference.

Figure 10 High levels of 32E03 in *A. thaliana* trigger RNA-directed DNA methylation of rDNA.

(A) Increased RNA polymerase II occupancy along the rDNA in *A. thaliana 32E03-H* line. Chromatin of wild type plants and the *32E03-H* line was immunoprecipitated with anti-RNA polymerase II antibodies, and rDNA regions shown in Figure 9A were qPCR-amplified. Wild type plants served as control. *Arabidopsis ACTIN 2* and *SN1* served as reference. The experiment was repeated three times, each with three technical replicates. Similar results were obtained from three independent experiments. Data from one representative experiment are shown. Data are the mean ± SE.
(B) Diagram showing *A. thaliana* rDNA regions. The indicated regions were amplified in C and D.
(C) Enhanced bidirectional transcription along the rDNA IGS in *32E03-H* line. cDNA of wild type plants and the *32E03-H* line was used to amplify the IGS regions indicated in B by RT-PCR and analyzed in 1% agarose gel electrophoresis. Wild type plants (WT) served as control. Band intensity of sense and anti-sense strand amplicons of each plant-type was quantified using the *ImageJ* software and the ratio is indicated in parenthesis. *Arabidopsis ACTIN 2* was amplified as reference. +/-RT, with or without reverse transcriptase.
(D) Enhanced rDNA IGS-specific small RNA biogenesis in *A. thaliana 32E03-H* line. Small RNA of wild type plants and the *32E03-H* line was resolved in a 15% TBE-urea gel, electroblotted, hybridized with siRNA probes as indicated in B and detected using Chemiluminescence Reagent. Wild type plants (WT) were used as control. Small nuclear RNA U6 (snRNA), loading control.
In C and D, the experiment was repeated at least two times. Similar results were obtained from the two independent experiments. Data from one representative experiment each are shown.
(E) Diagram highlighting the *A. thaliana* rDNA promoter analyzed by bisulphite sequencing (BS).
(F and G) *A. thaliana 32E03-H* line rDNA promoter is hypermethylated. (F) Analysis of cytosine methylation. Genomic DNA of wild type plants and the*32E03-H* line was digested with *BamHI* and

subjected to sodium bisulphite conversion. The rDNA promoter region indicated in E was amplified by PCR, cloned into pGEM-T Easy vector and analyzed by the CyMATE algorithm. Wild type plants were used as control. Approximately 25 promoter clones per genotype were analyzed.
(G) Percentage of cytosine methylation in wild-type plants and the *32E03-H* line in the three cytosine contexts. Total numbers of CG, CHG or CHH present in the rDNA promoter region are shown in parenthesis.
In A, C, D and F, plants of the tested genotypes were grown in a randomized block design. For each experiment, plants were sampled randomly to prepare pools for each genotype.

Figure 11 A subset of VAR1 rRNA variant is derepressed and VAR1:45S pre-rRNA ratio is altered in *A. thaliana 32E03-L* line.

(A) Expression of subtypes of rRNA variants in roots of *A. thaliana 32E03-L* line analyzed by SNP analysis. Wild type roots were used as control.
(B) Expression of subtypes of rRNA variants in *A. thaliana* wild-type root segments enriched in *H. schachtii*-induced syncytia analyzed by SNP analysis. Wild type plants were inoculated with *H. schachtii* J2s and root segments enriched in *H. schachtii*-induced syncytia (root+syncytium) and adjacent root segments without syncytia (root-syncytium; control) were dissected at 10 days post inoculation. In A and B, whole root or root segment cDNA was synthesized, subtypes of rRNA variants were amplified by PCR, gel-eluted, digested with *SphI*, *AluI* or *MspI* to detect VAR1-6645, VAR2-4302 or VAR3-7122 subtype, respectively. DNA fragments were visualized by 2.5% agarose gel electrophoresis. In A and B, the experiment comprised at least two biological replicates. Similar results were obtained in the two independent experiments. Data of one representative experiment are shown.
(C) Quantification of VAR1 rRNA and 45S pre-rRNA in *A. thaliana 32E03-L* line (14- and 18-days old) by qPCR. Wild type plants were used as control.
(D) Quantification of rRNA VAR1 and 45S pre-rRNA in wild-type *A. thaliana* root segments enriched in *H. schachtii*-induced syncytia by qPCR. Wild type plants were inoculated with *H. schachtii* J2s and root segments enriched in *H. schachtii*-induced syncytia (root+syncytium) and adjacent root segments without syncytia (root-syncytium; control) were dissected at 10 days post inoculation. In C and D, whole roots or root segments cDNA was synthesized, and VAR1 and 45S pre-RNA were quantified by qPCR. *ACTIN 8* was amplified as reference.
In C and D, the experiments comprised three biological replicates, each consisting of three technical replicates. Similar results were obtained in the three independent experiments. Data of one representative experiment are shown.
For A, B, C and D, plants of the tested genotypes/treatments were grown in randomized block designs. For each biological replicate, plants were sampled randomly to prepare pools for each genotype/treatment.

REFERENCES

Alvarez, M.E., Nota, F., and Cambiagno, D.A. (2010). Epigenetic control of plant immunity. Mol Plant Pathol **11,** 563-576.

Baum, T.J., Wubben, M.J., Hardyy, K.A., Su, H., and Rodermel, S.R. (2000). A Screen for Arabidopsis thaliana Mutants with Altered Susceptibility to Heterodera schachtii. J Nematol **32,** 166-173.

Becker, C., Hagmann, J., Muller, J., Koenig, D., Stegle, O., Borgwardt, K., and Weigel, D. (2011). Spontaneous epigenetic variation in the Arabidopsis thaliana methylome. Nature **480,** 245-249.

Berr, A., Menard, R., Heitz, T., and Shen, W.H. (2012). Chromatin modification and remodelling: a regulatory landscape for the control of Arabidopsis defence responses upon pathogen attack. Cellular microbiology **14,** 829-839.

Bourque, S., Dutartre, A., Hammoudi, V., Blanc, S., Dahan, J., Jeandroz, S., Pichereaux, C., Rossignol, M., and Wendehenne, D. (2011). Type-2 histone deacetylases as new regulators of elicitor-induced cell death in plants. New Phytol **192,** 127-139.

Brosch, G., Ramsom, R., Lechner, T., Walton, J.D., and Loidl, P. (1995). Inhibition of Maize Histone Deacetylases by Hc Toxin, the Host-Selective Toxin of Cochliobolus-Carbonum. Plant Cell **7,** 1941-1950.

Castillo-Gonzalez, C., Liu, X., Huang, C., Zhao, C., Ma, Z., Hu, T., Sun, F., Zhou, Y., Zhou, X., Wang, X.J., and Zhang, X. (2015). Geminivirus-encoded TrAP suppressor inhibits the histone methyltransferase SUVH4/KYP to counter host defense. eLife **4,** e06671.

Chandrasekhara, C., Mohannath, G., Blevins, T., Pontvianne, F., and Pikaard, C.S. (2016). Chromosome-specific NOR inactivation explains selective rRNA gene silencing and dosage control in Arabidopsis. Gene Dev **30,** 177-190.

Choi, S.M., Song, H.R., Han, S.K., Han, M., Kim, C.Y., Park, J., Lee, Y.H., Jeon, J.S., Noh, Y.S., and Noh, B. (2012). HDA19 is required for the repression of salicylic acid biosynthesis and salicylic acid-mediated defense responses in Arabidopsis. Plant J **71,** 135-146.

Clough, S.J., and Bent, A.F. (1998). Floral dip: a simplified method for Agrobacterium-mediated transformation of Arabidopsis thaliana. Plant J **16,** 735-743.

Colville, A., Alhattab, R., Hu, M., Labbe, H., Xing, T., and Miki, B. (2011). Role of HD2 genes in seed germination and early seedling growth in Arabidopsis. Plant cell reports **30,** 1969-1979.

Dahan, J., Hammoudi, V., Wendehenne, D., and Bourque, S. (2011). Type 2 histone deacetylases play a major role in the control of elicitor-induced cell death in tobacco. Plant signaling & behavior **6,** 1865-1867.

de Boer, J.M., Yan, Y., Smant, G., Davis, E.L., and Baum, T.J. (1998). In-situ hybridization to messenger RNA in Heterodera glycines. J Nematol **30,** 309-312.

Ding, B., and Wang, G.L. (2015). Chromatin versus pathogens: the function of epigenetics in plant immunity. Front Plant Sci **6,** 675.

Ding, B., Bellizzi, M.D., Ning, Y.S., Meyers, B.C., and Wang, G.L. (2012). HDT701, a Histone H4 Deacetylase, Negatively Regulates Plant Innate Immunity by Modulating Histone H4 Acetylation of Defense-Related Genes in Rice. Plant Cell **24,** 3783-3794.

Dowen, R.H., Pelizzola, M., Schmitz, R.J., Lister, R., Dowen, J.M., Nery, J.R., Dixon, J.E., and Ecker, J.R. (2012). Widespread dynamic DNA methylation in response to biotic stress. P Natl Acad Sci USA **109,** E2183-E2191.

Durut, N., Abou-Ellail, M., Pontvianne, F., Das, S., Kojima, H., Ukai, S., de Bures, A., Comella, P., Nidelet, S., Rialle, S., Merret, R., Echeverria, M., Bouvet, P., Nakamura, K., and Saez-Vasquez, J. (2014). A Duplicated NUCLEOLIN Gene with Antagonistic Activity Is Required for Chromatin Organization of Silent 45S rDNA in Arabidopsis. Plant Cell **26,** 1330-1344.

Earley, K.W., Pontvianne, F., Wierzbicki, A.T., Blevins, T., Tucker, S., Costa-Nunes, P., Pontes, O., and Pikaard, C.S. (2010). Mechanisms of HDA6-mediated rRNA gene silencing: suppression of intergenic Pol II transcription and differential effects on maintenance versus siRNA-directed cytosine methylation. Gene Dev **24,** 1119-1132.

Elling, A.A., Davis, E.L., Hussey, R.S., and Baum, T.J. (2007). Active uptake of cyst nematode parasitism proteins into the plant cell nucleus. Int J Parasitol **37,** 1269-1279.

Gao, B., Allen, R., Maier, T., Davis, E.L., Baum, T.J., and Hussey, R.S. (2001). Molecular characterisation and expression of two venom allergen-like protein genes in Heterodera glycines. Int J Parasitol **31,** 1617-1625.

Gao, B., Allen, R., Maier, T., Davis, E.L., Baum, T.J., and Hussey, R.S. (2003). The parasitome of the phytonematode Heterodera glycines. Molecular plant-microbe interactions : MPMI **16,** 720-726.

Grebenok, R.J., Pierson, E., Lambert, G.M., Gong, F.C., Afonso, C.L., HaldemanCahill, R., Carrington, J.C., and Galbraith, D.W. (1997). Green-fluorescent protein fusions for efficient characterization of nuclear targeting. Plant J **11,** 573-586.

Han, Z., Yu, H., Zhao, Z., Hunter, D., Luo, X., Duan, J., and Tian, L. (2016). AtHD2D Gene Plays a Role in Plant Growth, Development, and Response to Abiotic Stresses in Arabidopsis thaliana. Front Plant Sci **7,** 310.

Hermsmeier, D., Hart, J.K., Byzova, M., Rodermel, S.R., and Baum, T.J. (2000). Changes in mRNA abundance within Heterodera schachtii-infected roots of Arabidopsis thaliana. Molecular plant-microbe interactions : MPMI **13,** 309-315.

Hetzl, J., Foerster, A.M., Raidl, G., and Scheid, O.M. (2007). CyMATE: a new tool for methylation analysis of plant genornic DNA after bisulphite sequencing. Plant J **51,** 526-536.

Hewezi, T., and Baum, T.J. (2013). Manipulation of Plant Cells by Cyst and Root-Knot Nematode Effectors. Mol Plant Microbe In **26,** 9-16.

Hewezi, T., Howe, P., Maier, T.R., Hussey, R.S., Mitchum, M.G., Davis, E.L., and Baum, T.J. (2008). Cellulose Binding Protein from the Parasitic Nematode Heterodera schachtii Interacts with Arabidopsis Pectin Methylesterase: Cooperative Cell Wall Modification during Parasitism. Plant Cell **20,** 3080-3093.

Hewezi, T., Howe, P.J., Maier, T.R., Hussey, R.S., Mitchum, M.G., Davis, E.L., and Baum, T.J. (2010). Arabidopsis spermidine synthase is targeted by an effector protein of the cyst nematode Heterodera schachtii. Plant Physiol **152,** 968-984.

Hewezi, T., Juvale, P.S., Piya, S., Maier, T.R., Rambani, A., Rice, J.H., Mitchum, M.G., Davis, E.L., Hussey, R.S., and Baum, T.J. (2015). The Cyst Nematode Effector Protein 10A07 Targets and Recruits Host Posttranslational Machinery to Mediate Its Nuclear Trafficking and to Promote Parasitism in Arabidopsis. Plant Cell **27,** 891-907.

Jefferson, R.A., Kavanagh, T.A., and Bevan, M.W. (1987). Gus Fusions - Beta-Glucuronidase as a Sensitive and Versatile Gene Fusion Marker in Higher-Plants. Embo J **6,** 3901-3907.

Kankel, M.W., Ramsey, D.E., Stokes, T.L., Flowers, S.K., Haag, J.R., Jeddeloh, J.A., Riddle, N.C., Verbsky, M.L., and Richards, E.J. (2003). Arabidopsis MET1 cytosine methyltransferase mutants. Genetics **163,** 1109-1122.

Kim, K.C., Lai, Z., Fan, B., and Chen, Z. (2008). Arabidopsis WRKY38 and WRKY62 transcription factors interact with histone deacetylase 19 in basal defense. Plant Cell **20,** 2357-2371.

Kong, L., Qiu, X., Kang, J., Wang, Y., Chen, H., Huang, J., Qiu, M., Zhao, Y., Kong, G., Ma, Z., Wang, Y., Ye, W., Dong, S., Ma, W., and Wang, Y. (2017). A Phytophthora Effector Manipulates Host Histone Acetylation and Reprograms Defense Gene Expression to Promote Infection. Current biology : CB **27,** 981-991.

Lawrence, R.J., Earley, K., Pontes, O., Silva, M., Chen, Z.J., Neves, N., Viegas, W., and Pikaard, C.S. (2004). A concerted DNA methylation/histone methylation switch regulates rRNA gene dosage control and nucleolar dominance. Mol Cell **13,** 599-609.

Li, H., and Luan, S. (2010). AtFKBP53 is a histone chaperone required for repression of ribosomal RNA gene expression in Arabidopsis. Cell Res **20,** 357-366.

Lindroth, A.M., Cao, X.F., Jackson, J.P., Zilberman, D., McCallum, C.M., Henikoff, S., and Jacobsen, S.E. (2001). Requirement of CHROMOMETHYLASE3 for maintenance of CpXpG methylation. Science **292,** 2077-2080.

Lister, R., O'Malley, R.C., Tonti-Filippini, J., Gregory, B.D., Berry, C.C., Millar, A.H., and Ecker, J.R. (2008). Highly integrated single-base resolution maps of the epigenome in Arabidopsis. Cell **133,** 523-536.

Livak, K.J., and Schmittgen, T.D. (2001). Analysis of relative gene expression data using real-time quantitative PCR and the 2(-Delta Delta C(T)) Method. Methods **25,** 402-408.

Luo, M., Wang, Y.Y., Liu, X.C., Yang, S.G., Lu, Q., Cui, Y.H., and Wu, K.Q. (2012). HD2C interacts with HDA6 and is involved in ABA and salt stress response in Arabidopsis. J Exp Bot **63,** 3297-3306.

Matzke, N.J. (2016). The evolution of antievolution policies after Kitzmiller versus Dover. Science **351,** 28-30.

Mitchum, M.G., Hussey, R.S., Baum, T.J., Wang, X.H., Elling, A.A., Wubben, M., and Davis, E.L. (2013). Nematode effector proteins: an emerging paradigm of parasitism. New Phytol **199,** 879-894.

Murfett, J., Wang, X.J., Hagen, G., and Guilfoyle, T.J. (2001). Identification of Arabidopsis histone deacetylase HDA6 mutants that affect transgene expression. Plant Cell **13,** 1047-1061.

Nakai, K., and Horton, P. (1999). PSORT: a program for detecting sorting signals in proteins and predicting their subcellular localization. Trends Biochem Sci **24,** 34-35.

Olias, P., Etheridge, R.D., Zhang, Y., Holtzman, M.J., and Sibley, L.D. (2016). Toxoplasma Effector Recruits the Mi-2/NuRD Complex to Repress STAT1 Transcription and Block IFN-gamma-Dependent Gene Expression. Cell Host Microbe **20,** 72-82.

Pogorelko, G., Juvale, P.S., Rutter, W.B., Hewezi, T., Hussey, R., Davis, E.L., Mitchum, M.G., and Baum, T.J. (2016). A cyst nematode effector binds to diverse plant proteins, increases nematode susceptibility and affects root morphology. Mol Plant Pathol **17,** 832-844.

Pontes, O., Lawrence, R.J., Silva, M., Preuss, S., Costa-Nunes, P., Earley, K., Neves, N., Viegas, W., and Pikaard, C.S. (2007). Postembryonic Establishment of Megabase-Scale Gene Silencing in Nucleolar Dominance. Plos One **2**.

Pontvianne, F., Blevins, T., Chandrasekhara, C., Feng, W., Stroud, H., Jacobsen, S.E., Michaels, S.D., and Pikaard, C.S. (2012). Histone methyltransferases regulating rRNA gene dose and dosage control in Arabidopsis. Gene Dev **26,** 945-957.

Pontvianne, F., Blevins, T., Chandrasekhara, C., Mozgova, I., Hassel, C., Pontes, O.M.F., Tucker, S., Mokros, P., Muchova, V., Fajkus, J., and Pikaard, C.S. (2013). Subnuclear partitioning of rRNA genes between the nucleolus and nucleoplasm reflects alternative epiallelic states. Gene Dev **27,** 1545-1550.

Pontvianne, F., Abou-Ellail, M., Douet, J., Comella, P., Matia, I., Chandrasekhara, C., DeBures, A., Blevins, T., Cooke, R., Medina, F.J., Tourmente, S., Pikaard, C.S., and Saez-Vasquez, J. (2010). Nucleolin Is Required for DNA Methylation State and the Expression of rRNA Gene Variants in Arabidopsis thaliana. Plos Genet **6**.

Rambani, A., Rice, J.H., Liu, J., Lane, T., Ranjan, P., Mazarei, M., Pantalone, V., Stewart, C.N., Jr., Staton, M., and Hewezi, T. (2015). The Methylome of Soybean Roots during the Compatible Interaction with the Soybean Cyst Nematode. Plant Physiol **168,** 1364-1377.

Ransom, R.F., and Walton, J.D. (1997). Histone hyperacetylation in maize in response to treatment with HC-toxin or infection by the filamentous fungus Cochliobolus carbonum. Plant Physiol **115,** 1021-1027.

Rolando, M., Sanulli, S., Rusniok, C., Gomez-Valero, L., Bertholet, C., Sahr, T., Margueron, R., and Buchrieser, C. (2013). Legionella pneumophila Effector RomA Uniquely Modifies Host Chromatin to Repress Gene Expression and Promote Intracellular Bacterial Replication. Cell Host Microbe **13,** 395-405.

Schmitz, R.J., Schultz, M.D., Lewsey, M.G., O'Malley, R.C., Urich, M.A., Libiger, O., Schork, N.J., and Ecker, J.R. (2011). Transgenerational Epigenetic Instability Is a Source of Novel Methylation Variants. Science **334,** 369-373.

Sijmons, P.C., Grundler, F.M.W., Vonmende, N., Burrows, P.R., and Wyss, U. (1991). Arabidopsis-Thaliana as a New Model Host for Plant-Parasitic Nematodes. Plant J **1,** 245-254.

Sindhu, A., Chintamanani, S., Brandt, A.S., Zanis, M., Scofield, S.R., and Johal, G.S. (2008). A guardian of grasses: specific origin and conservation of a unique disease-resistance gene in the grass lineage. Proc Natl Acad Sci U S A **105,** 1762-1767.

Sukno, S.A., McCuiston, J., Wong, M.Y., Wang, X.H., Thon, M.R., Hussey, R., Baum, T., and Davis, E. (2007). Quantitative detection of double-stranded RNA-mediated gene silencing of parasitism genes in Heterodera glycines. J Nematol **39,** 145-152.

Wierzbicki, A.T., Haag, J.R., and Pikaard, C.S. (2008). Noncoding Transcription by RNA Polymerase Pol IVb/Pol V Mediates Transcriptional Silencing of Overlapping and Adjacent Genes. Cell **135,** 635-648.

Wight, W.D., Kim, K.H., Lawrence, C.B., and Walton, J.D. (2009). Biosynthesis and role in virulence of the histone deacetylase inhibitor depudecin from Alternaria brassicicola. Molecular plant-microbe interactions : MPMI **22,** 1258-1267.

Yang, L., Li, B.S., Zheng, X.Y., Li, J.G., Yang, M., Dong, X.N., He, G.M., An, C.C., and Deng, X.W. (2015). Salicylic acid biosynthesis is enhanced and contributes to increased biotrophic pathogen resistance in Arabidopsis hybrids. Nat Commun **6**.

Yang, W.M., Yao, Y.L., and Seto, E. (2001). The FK506-binding protein 25 functionally associates with histone deacetylases and with transcription factor YY1. Embo J **20,** 4814-4825.

Yano, R., Takebayashi, Y., Nambara, E., Kamiya, Y., and Seo, M. (2013). Combining association mapping and transcriptomics identify HD2B histone deacetylase as a genetic factor associated with seed dormancy in Arabidopsis thaliana. Plant J **74,** 815-828.

Yu, A., Lepere, G., Jay, F., Wang, J.Y., Bapaume, L., Wang, Y., Abraham, A.L., Penterman, J., Fischer, R.L., Voinnet, O., and Navarro, L. (2013). Dynamics and biological relevance of DNA demethylation in Arabidopsis antibacterial defense. P Natl Acad Sci USA **110,** 2389-2394.

Zhang, L., Davies, L.J., and Elling, A.A. (2015). A Meloidogyne incognita effector is imported into the nucleus and exhibits transcriptional activation activity in planta. Mol Plant Pathol **16,** 48-60.

Zhao, J.H., Zhang, J.X., Zhang, W., Wu, K.L., Zheng, F., Tian, L.N., Liu, X.C., and Duan, J. (2015). Expression and functional analysis of the plant-specific histone deacetylase HDT701 in rice. Front Plant Sci **5**.

Zhou, C.H., Zhang, L., Duan, J., Miki, B., and Wu, K.Q. (2005). HISTONE DEACETYLASE19 is involved in jasmonic acid and ethylene signaling of pathogen response in Arabidopsis. Plant Cell **17,** 1196-1204.

Zhu, Q.H., Shan, W.X., Ayliffe, M.A., and Wang, M.B. (2016). Epigenetic Mechanisms: An Emerging Player in Plant-Microbe Interactions. Molecular plant-microbe interactions : MPMI **29,** 187-196.

Zilberman, D., Gehring, M., Tran, R.K., Ballinger, T., and Henikoff, S. (2007). Genome-wide analysis of Arabidopsis thaliana DNA methylation uncovers an interdependence between methylation and transcription. Nat Genet **39,** 61-69.

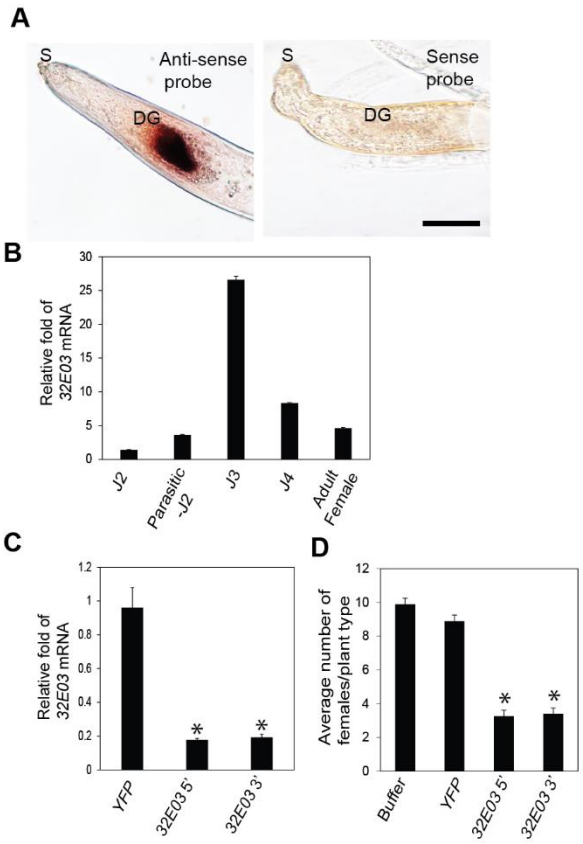

Figure 1 *H. schachtii* effector *32E03* has important pathogenicity function.

(A) *32E03* mRNA is abundantly expressed in the dorsal esophageal gland (DG) of *H. schachtii*. *In situ* hybridization of digoxigenin-labeled *32E03* antisense- or sense-cDNA probes to *32E03* transcripts expressed in the DG of third-stage (J3) nematodes. S, stylet; Scale bar = 10 µm.
(B) *32E03* mRNA is detectable throughout the life cycle of *H. schachtii*. Total RNA was extracted from eggs, second-stage (J2), third-stage (J3), fourth-stage (J4) and adult female nematodes. cDNA was synthesized, and abundance of *32E03* mRNA was quantified by qPCR in each life stage in three technical replicates. *β-ACTIN* mRNA abundance was used to normalize *32E03* expression. The fold values indicate values relative to that of eggs ± SE.
(C-D) RNAi of *32E03* expression in *H. schachtii* inhibits pathogenicity. (C) Downregulation of *32E03* expression in RNAi *H. schachtii*. Pools of newly hatched *H. schachtii* J2 nematodes were soaked in *32E03* double-stranded RNA (dsRNA), *yellow fluorescent protein* (YFP) dsRNA or only buffer. Total RNA of nematode pools was extracted, cDNA was synthesized and abundance of *32E03* was quantified by qPCR. *β-ACTIN* mRNA abundance was used to normalize *32E03* expression. Expression values are shown as fold changes relative to nematodes soaked in buffer. The experiment was repeated three times, each with three technical replicates. Similar results were obtained from three independent experiments and only data from one representative experiment are shown. Shown data are means ± SE. 5' or 3' indicates 5' or 3' region of the *32E03* mRNA, respectively. Mean values significantly different from that of nematodes soaked in buffer were determined by unadjusted paired *t*-test and are indicated by an asterisk (P<0.1%).
(D) Downregulation of *32E03* expression in *H. schachtii* inhibits pathogenicity. *A. thaliana* wild type plants were inoculated with RNAi nematodes or nematodes soaked in buffer, and 4 weeks after inoculation, the number of adult females per plant was determined. Data are the average number of adult females ± SE (n = 30). The experiment was repeated at least three times. Similar results were obtained from three independent experiments. Data from one representative experiment are shown. Mean values significantly different from that of the nematode soaked in buffer were determined by unadjusted paired *t*-tests (P < 0.05) using the *SAS* statistical software package and are indicated by an asterisk.

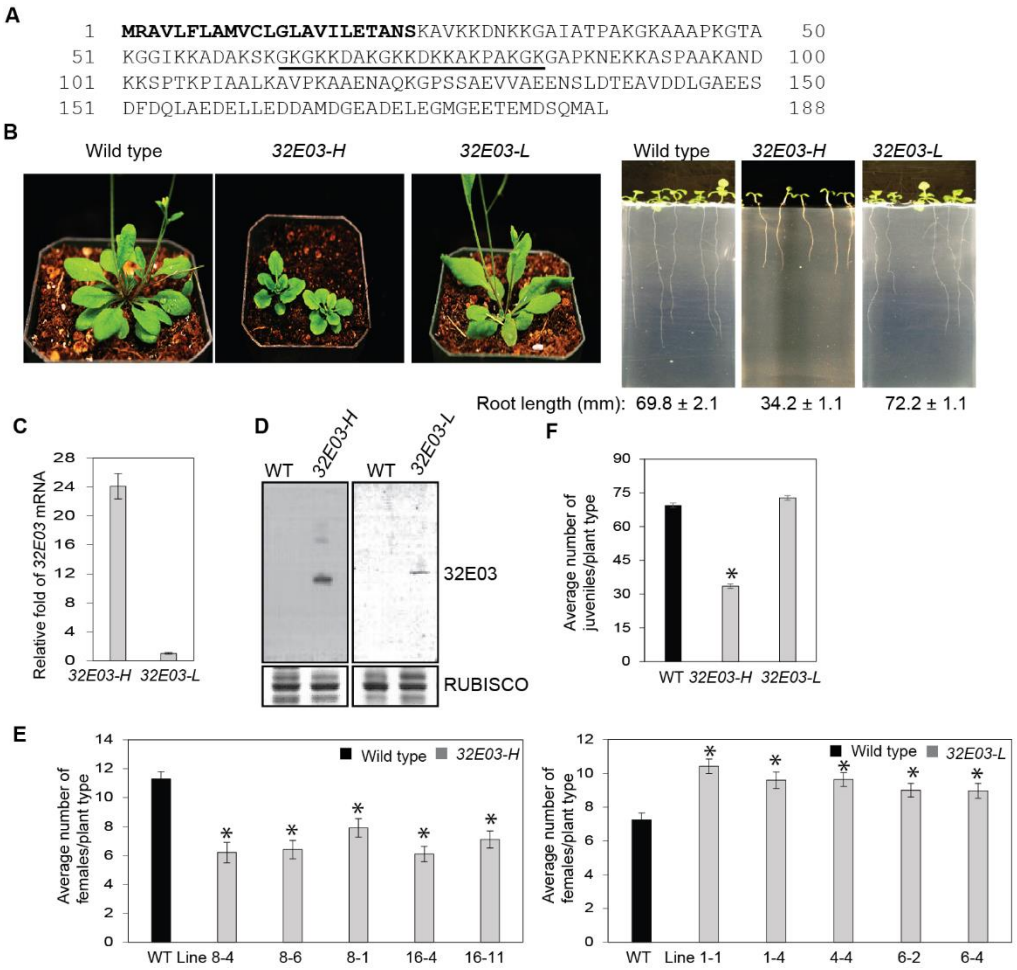

Figure 2 Expression of 32E03 in *A. thaliana* alters morphology and susceptibility to *H. schachtii*.

(A) Amino acid sequence of 32E03 effector of *H. schachtii*. N-terminus of 32E03 contains a secretory signal peptide (in bold). Bipartite nuclear localization signal predicted by PSORT algorithm is underlined.
(B) Morphology of transgenic *A. thaliana* plants expressing 32E03. *A. thaliana* wild type plants were transformed with a construct containing the *32E03* coding sequence without the secretory signal peptide under control of the *35S* promoter. In the T3 generation, two types of homozygous lines (*32E03-H* and *32E03-L*) varying in morphology were identified. Root length is the average measurement of 20 plant roots ± SE.
(C) Quantification of *32E03* mRNA in transgenic *A. thaliana* lines. Total RNA of *A. thaliana 32E03-H* and *32E03-L* lines was extracted and the levels of *32E03* mRNA were quantified by qPCR. *ACTIN 2* was amplified as reference. Data are the mean ± SE. The experiment consisted of three independent biological replicates, each encompassing three technical replicates.
(D) Quantification of 32E03 protein in transgenic *A. thaliana* lines. Total protein of *A. thaliana 32E03-H* and *32E03-L* lines was resolved in Novex 4-16% Tris-glycine SDS-PAGE, electroblotted onto a PVDF membrane, probed with anti-32E03 antibodies and detected using LumiSensor Chemiluminescent HRP Substrate. RUBISCO was detected as loading control.
(E) Expression of 32E03 in *A. thaliana* plant affects susceptibility to *H. schachtii*. Five independent *A. thaliana 32E03-H* and *32E03-L* lines each were inoculated with *H. schachtii* J2 nematodes, and four weeks after inoculation, the number of adult females per plant were counted. *H. schachtii*-inoculated *A. thaliana* wild type plant was used as control. Each experiment was repeated three times. Data are the average of adult females per plant in each plant type ± SE (n = 30). Mean values significantly different

from that of wild-type plants were determined by unadjusted paired *t*-tests ($P < 0.05$) using the *SAS* statistical software package and are indicated by an asterisk.
(F) Root penetration by *H. schachtii* juveniles is reduced in *A. thaliana 32E03-H* line. *A. thaliana 32E03-H* and *32E03-L* lines were inoculated with *H. schachtii* J2 nematodes, and four days of post inoculation, the number of nematodes that had penetrated into each plant-type was counted. *H. schachtii* inoculated wild type plants were used as control. The experiment comprised three independent *32E03-H* and *32E03-L* lines each. Data are the average number of penetrated nematodes in each plant type ± SE ($n = 16$). Mean values significantly different from that of wild-type plants were determined by unadjusted paired *t*-tests ($P < 0.05$) using the *SAS* statistical software package and are indicated by an asterisk.

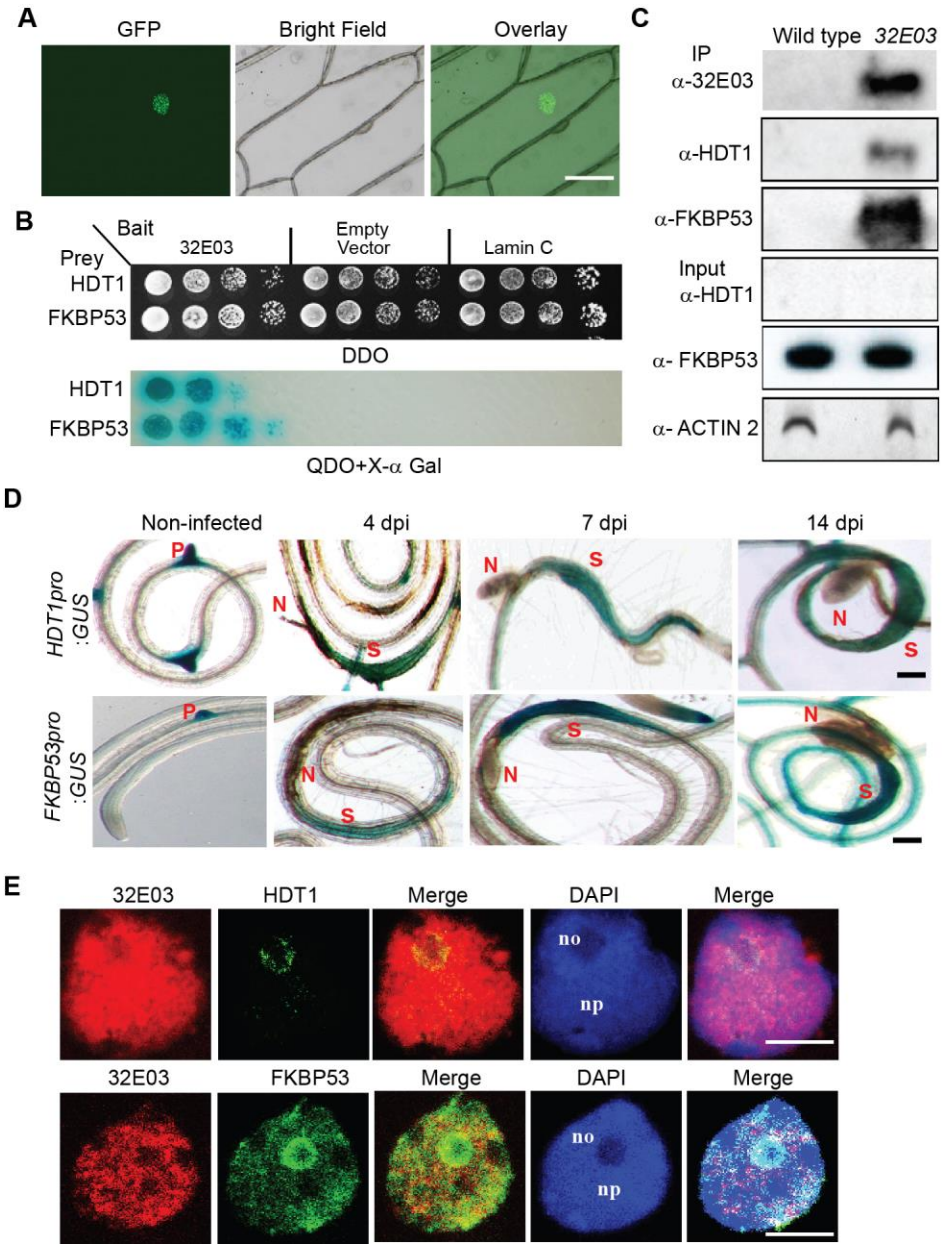

Figure 3 32E03 expressed in *A. thaliana* interacts and co-localizes with HDT1 and FKBP53 proteins.

(A) 32E03 accumulates in the plant nucleus. A plasmid containing the *32E03* coding sequence without the secretory signal peptide fused to the *GFP-GUS* gene was delivered into onion epidermal cells using biolistic bombardment, and the bombarded cells were analyzed by epifluorescence microscopy. Bar = 100 µm.
(B) 32E03 interacts with *A. thaliana* HDT1 and FKBP53 in yeast. Yeast cells co-transformed with the *32E03* bait plasmid and the *HDT1* or *FKBP53* prey plasmid were grown on a low stringency double dropout (DDO) medium and a high stringency quadruple dropout (QDO) medium in the presence of X-α Gal to confirm protein interaction. Empty prey vector or prey vector containing human *Lamin C* served as controls.
(C) 32E03 synthesized in *A. thaliana* forms a complex with endogenous HDT1 and FKBP53. Nuclear extract of a 32E03-expressing *A. thaliana* line was immunoprecipitated with anti-32E03 antibodies, and the immunoprecipitates (IP) were analyzed by protein gel blot using anti-32E03, anti-HDT1 or anti-

FKBP53 antibodies. HDT1, FKBP53 and ACTIN 2 in input nuclear extract was detected as loading control.
(D) *H. schachtii* infection upregulates *A. thaliana HDT1* and *FKBP53* promoter activities. *A. thaliana* transgenic plants harboring the *GUS* gene under the control of the *HDT1* (*HDT1pro:GUS*) or *FKBP53* (*FKBP53pro:GUS*) promoter were inoculated with *H. schachtii*, and the infected roots were analyzed for GUS expression by histochemical assays. dpi, days post inoculation. N, nematode; S, syncytium; P, lateral root primordium. Scale bar = 10 μm.
(E) 32E03 co-localizes with endogenous *A. thaliana* HDT1 and FKBP53. Nuclei of 32E03-expressing *A. thaliana* line were immunostained with anti-32E03 antibodies in combination with anti-HDT1 or anti-FKBP53 antibodies, probed with secondary antibodies conjugated to Alexa Fluor 488 or Alexa Fluor 594 and counterstained with 4', 6-diamidino-2-phenylindole (DAPI). About 200 nuclei in each preparation were analyzed by confocal microscopy. no, nucleolus; np, nucleoplasm. Scale bar = 5 mm.

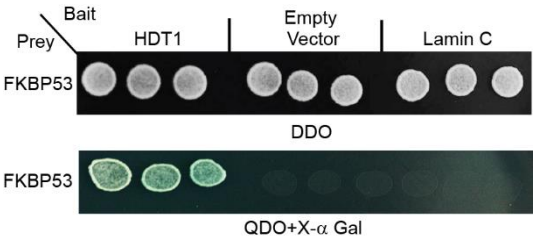

Figure 4 *A. thaliana* HDT1 and FKBP53 interact.
Yeast cells co-transformed with the *HDT1* bait plasmid and the *FKBP53* prey plasmid were grown on a low stringency double dropout (DDO) medium and a high stringency quadruple dropout (QDO) medium in the presence of X-α Gal to confirm protein interaction. Empty prey vector or prey vector containing human *Lamin C* served as controls.

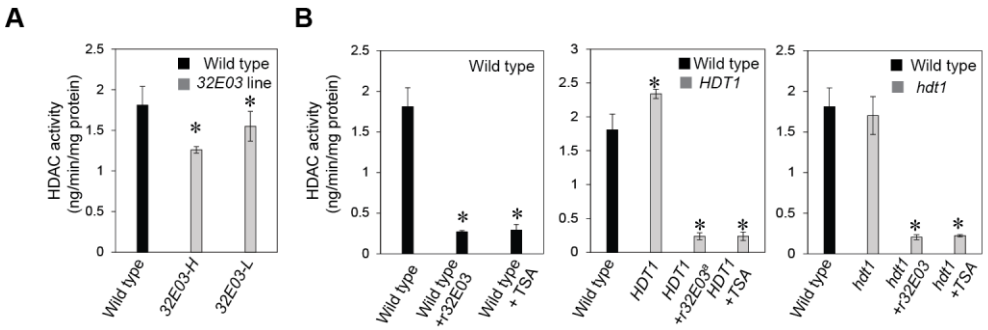

Figure 5 32E03 inhibits histone deacetylase (HDAC) activities.

(A) Expression of 32E03 in *A. thaliana* inhibits HDAC activities. HDAC activities of the *32E03-H* and *32E03-L* lines were compared to that of the wild type plants.
(B) Recombinant 32E03 inhibits HDAC activities. HDAC activities in the wild type, *HDT1* and *hdt1* plants were measured in the presence or absence of recombinant 32E03 protein (r32E03; 500 or 1500[a] nM) or trichostatin (TSA, 500 nM).
In A and B, plants of the tested genotypes were grown in a randomized block design. For each biological replicate, plants were sampled randomly to prepare pools for each line. Nuclei of *A. thaliana* pools were isolated and nuclear extracts were prepared for HDAC assays. The experiment comprised three biological replicates, each with three technical replicates. Data are the mean values ± SE. Statistically significant changes in HDAC activity were determined by unadjusted paired *t*-test and are indicated by an asterisk (P≤0.1).

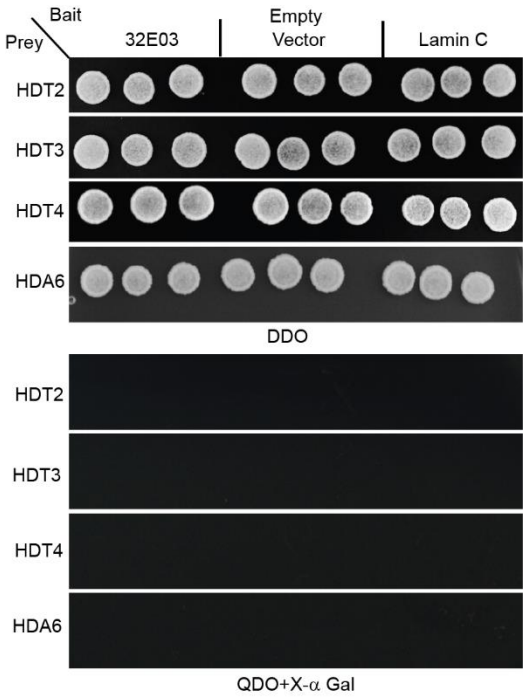

Figure 6 32E03 does not interact with other tuin-type histone deacetylases or HDA6 of *A. thaliana* in Y2H system.

Yeast cells co-transformed with the *32E03* bait plasmid and the *HDT2, HDT3, HDT4* or *HDA6* prey plasmid were grown on a low stringency double dropout (DDO) medium and a high stringency quadruple dropout (QDO) medium in the presence of X-α Gal to confirm protein interaction. Empty prey vector or prey vector containing human *Lamin C* served as controls.

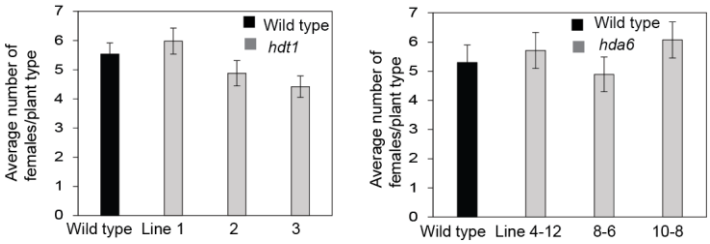

Figure 7 Susceptibility to *H. schachtii* is not altered in *A. thaliana hdt1* and *hda6* lines.

Three independent lines of *A. thaliana hdt1* and *hda6* each were inoculated with *H. schachtii* J2 nematodes, and four weeks after inoculation, the number of adult females per plant were counted. *H. schachtii*-inoculated *A. thaliana* wild type plants were used as control. The experiment was repeated three times. Similar results were obtained in three independent experiments. Data of one representative experiment are shown. Data are the average of adult females per plant in each plant-type ± SE (n = 30). Mean values significantly different from that of wild-type plants were determined by unadjusted paired *t*-tests ($P < 0.05$) using the *SAS* statistical software package.

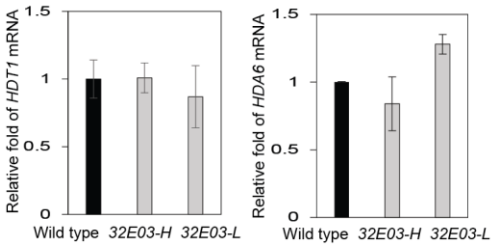

Figure 8 Expression of *HDT1* and *HDA6* is unaltered in A*. thaliana 32E03-H* and *32E03-L* lines.

Root total RNA of *A. thaliana* wild type plants and the *32E03-H* and *32E03-L* lines was extracted, cDNA was synthesized and *HDT1* and *HDA6* expression was quantified by qPCR. Wild type plants were used as control. *ACTIN 2* was amplified as reference. Tested genotypes were grown in randomized block designs. For each biological replicate, plants were sampled randomly to prepare pools for each genotype. The experiment consisted of three biological replicates, each encompassing three technical replicates. Data are the mean ± SE. Statistically significant difference in the mean values was analyzed by unadjusted paired *t*-test (P=0.05).

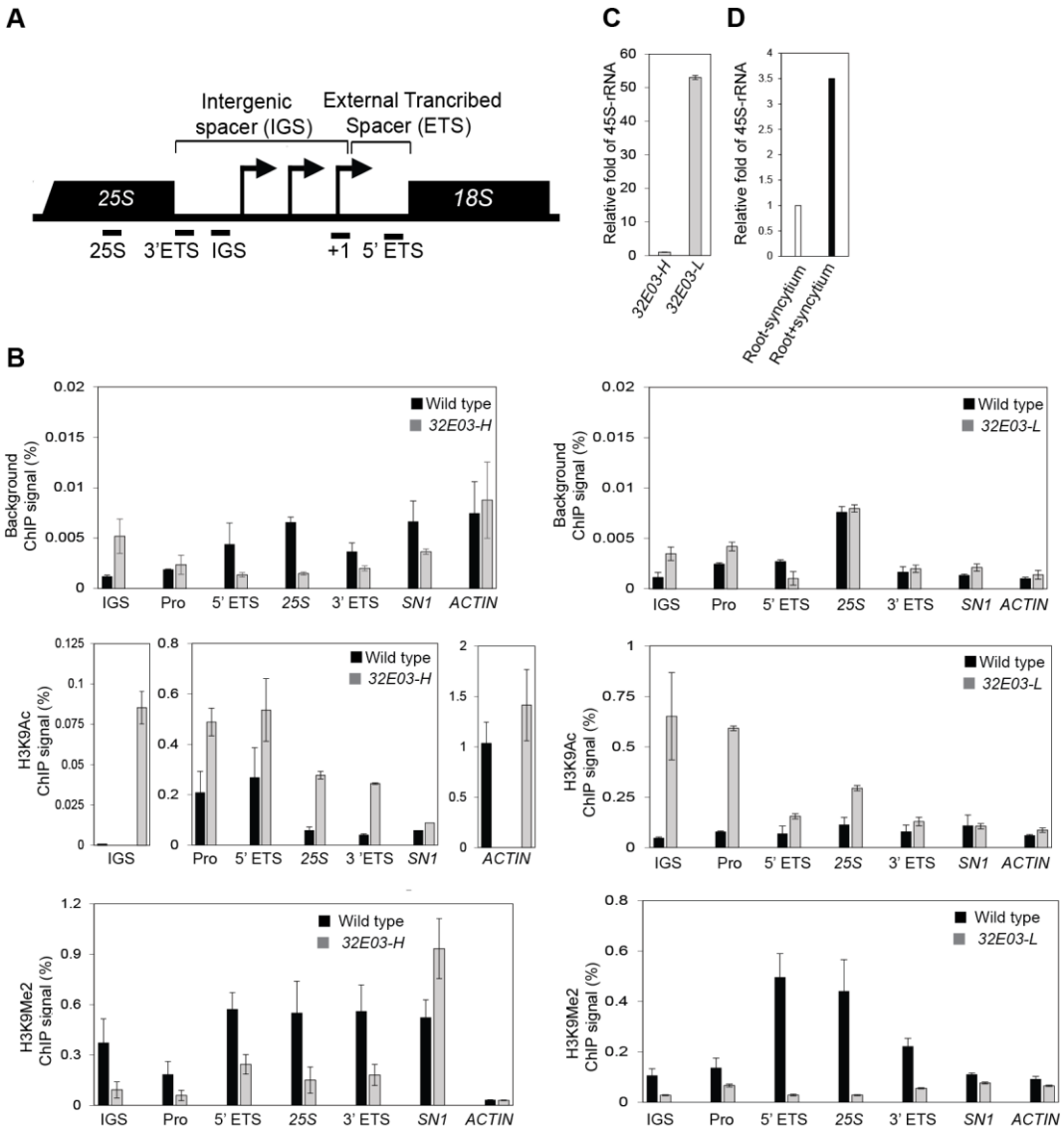

Figure 9 Expression of the *32E03* coding sequence in *A. thaliana* mediates rDNA chromatin modifications and alters 45S pre-rRNA abundance.

(A) Diagram showing *A. thaliana* rDNA regions. The indicated regions were amplified in qPCR assays shown in Figure 9B, 10A and Supplemental Figure 3A. *25S* and *18S*, coding region; +1, transcription start site.
(B) 32E03 expression in *A. thaliana* causes histone H3 modifications along the rDNA. Chromatin of *32E03-H* and *32E03-L* lines was immunoprecipitated with anti-H3K9Ac or anti-H3K9me2 antibodies and subjected to qPCR to quantify the rDNA regions indicated in A. Wild type plants were used as control. *ACTIN 2* and *SN1* were amplified as reference. Pro, promoter.
(C) Abundance of 45S pre-rRNA in *A. thaliana 32E03-H* and *32E03-L* lines. Total RNA of roots of *A. thaliana* wild type plants and *32E03-H* and *32E03-L* lines was extracted. Wild-type plants were used as control. 45S pre-rRNA in the 32E03 expression lines was determined relative to wild-type plants.
(D) Abundance of 45S pre-rRNA in *A. thaliana* wild-type root segments enriched in *H. schachtii*-induced syncytia. Wild type plants were inoculated with *H. schachtii* J2s. Root segments enriched in *H. schachtii*-induced syncytia (root+syncytium) and adjacent root segments without syncytia (root-syncytia; control) were dissected at 10 days post inoculation.

For B, C and D, plants of the tested genotypes/treatments were grown in randomized block designs. For each biological replicate, plants were sampled randomly to prepare pools for each genotype/treatment. Experiments comprised three biological replicates, each with three technical replicates. Similar results were obtained from three independent experiments. Data from one representative experiment each are shown in B, C, and D. Data are the means ± SE.
For C and D, root cDNA was synthesized and 45S pre-rRNA was quantified by qPCR. *Arabidopsis ACTIN 8* was amplified as reference.

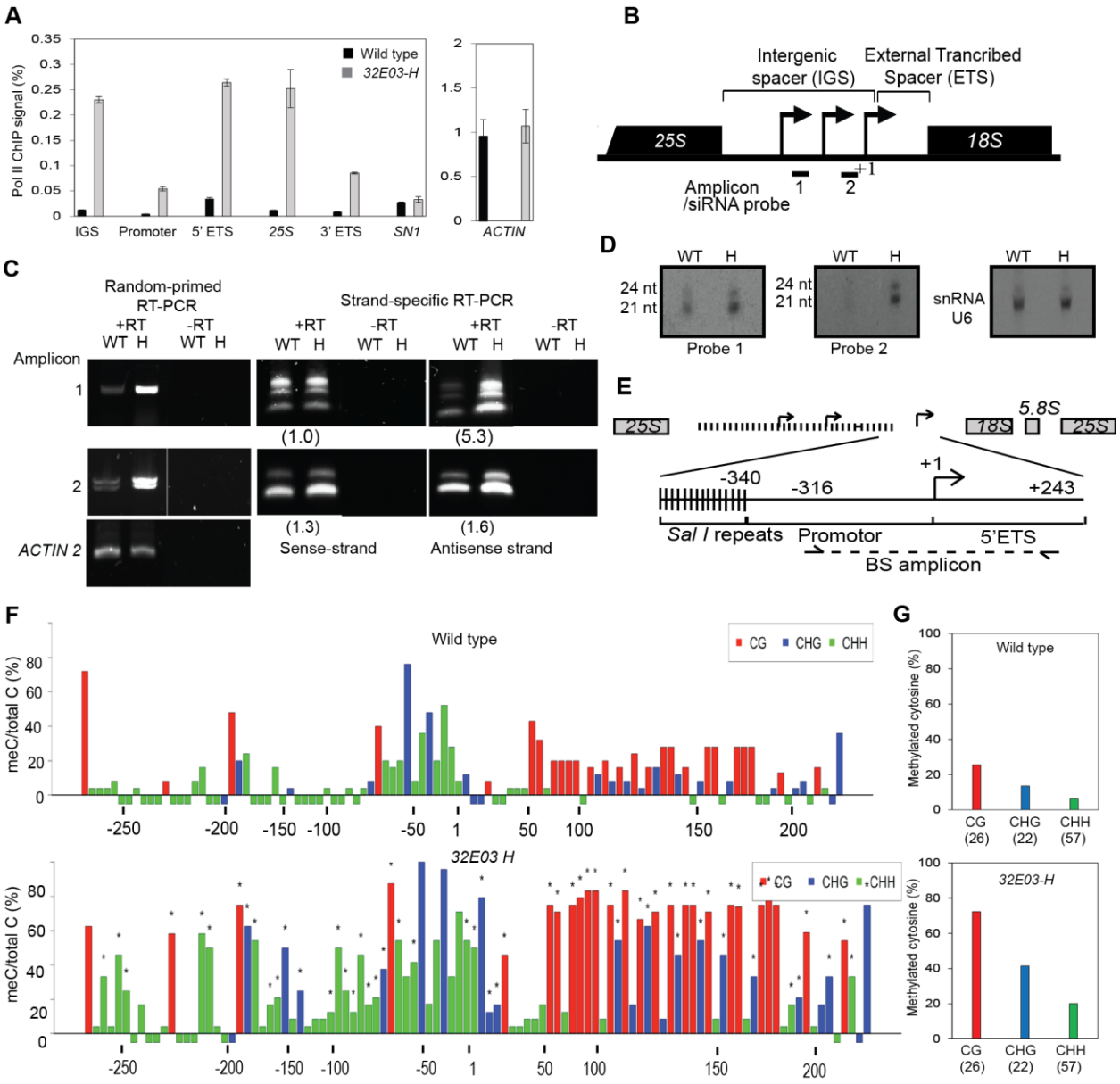

Figure 10 High levels of 32E03 in *A. thaliana* trigger RNA-directed DNA methylation of rDNA.

(A) Increased RNA polymerase II occupancy along the rDNA in *A. thaliana 32E03-H* line. Chromatin of wild type plants and the *32E03-H* line was immunoprecipitated with anti-RNA polymerase II antibodies, and rDNA regions shown in Figure 9A were qPCR-amplified. Wild type plants served as control. *Arabidopsis ACTIN 2* and *SN1* served as reference. The experiment was repeated three times, each with three technical replicates. Similar results were obtained from three independent experiments. Data from one representative experiment are shown. Data are the mean ± SE.
(B) Diagram showing *A. thaliana* rDNA regions. The indicated regions were amplified in C and D.
(C) Enhanced bidirectional transcription along the rDNA IGS in *32E03-H* line. cDNA of wild type plants and the *32E03-H* line was used to amplify the IGS regions indicated in B by RT-PCR and analyzed in 1% agarose gel electrophoresis. Wild type plants (WT) served as control. Band intensity of sense and anti-sense strand amplicons of each plant-type was quantified using the *ImageJ* software and the ratio is indicated in parenthesis. *Arabidopsis ACTIN 2* was amplified as reference. +/-RT, with or without reverse transcriptase.

(D) Enhanced rDNA IGS-specific small RNA biogenesis in *A. thaliana 32E03-H* line. Small RNA of wild type plants and the *32E03-H* line was resolved in a 15% TBE-urea gel, electroblotted, hybridized with siRNA probes as indicated in B and detected using Chemiluminescence Reagent. Wild type plants (WT) were used as control. Small nuclear RNA U6 (snRNA), loading control.
In C and D, the experiment was repeated at least two times. Similar results were obtained from the two independent experiments. Data from one representative experiment each are shown.
(E) Diagram highlighting the *A. thaliana* rDNA promoter analyzed by bisulphite sequencing (BS).
(F and G) *A. thaliana 32E03-H* line rDNA promoter is hypermethylated. (F) Analysis of cytosine methylation. Genomic DNA of wild type plants and the*32E03-H* line was digested with *BamHI* and subjected to sodium bisulphite conversion. The rDNA promoter region indicated in E was amplified by PCR, cloned into pGEM-T Easy vector and analyzed by the CyMATE algorithm. Wild type plants were used as control. Approximately 25 promoter clones per genotype were analyzed.
(G) Percentage of cytosine methylation in wild-type plants and the *32E03-H* line in the three cytosine contexts. Total numbers of CG, CHG or CHH present in the rDNA promoter region are shown in parenthesis.
In A, C, D and F, plants of the tested genotypes were grown in a randomized block design. For each experiment, plants were sampled randomly to prepare pools for each genotype.

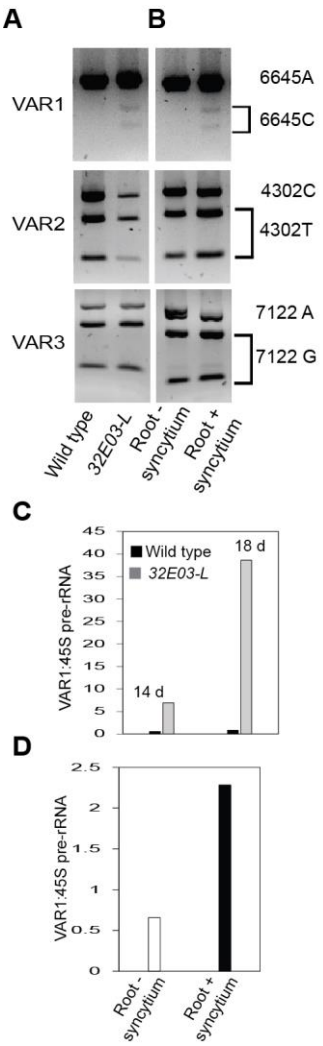

Figure 11 A subset of VAR1 rRNA variant is derepressed and VAR1:45S pre-rRNA ratio is altered in *A. thaliana 32E03-L* line.

(A) Expression of subtypes of rRNA variants in roots of *A. thaliana 32E03-L* line analyzed by SNP analysis. Wild type roots were used as control.
(B) Expression of subtypes of rRNA variants in *A. thaliana* wild-type root segments enriched in *H. schachtii*-induced syncytia analyzed by SNP analysis. Wild type plants were inoculated with *H. schachtii* J2s and root segments enriched in *H. schachtii*-induced syncytia (root+syncytium) and adjacent root segments without syncytia (root-syncytium; control) were dissected at 10 days post inoculation. In A and B, whole root or root segment cDNA was synthesized, subtypes of rRNA variants were amplified by PCR, gel-eluted, digested with *SphI*, *AluI* or *MspI* to detect VAR1-6645, VAR2-4302 or VAR3-7122 subtype, respectively. DNA fragments were visualized by 2.5% agarose gel electrophoresis. In A and B, the experiment comprised at least two biological replicates. Similar results were obtained in the two independent experiments. Data of one representative experiment are shown.
(C) Quantification of VAR1 rRNA and 45S pre-rRNA in *A. thaliana 32E03-L* line (14- and 18-days old) by qPCR. Wild type plants were used as control.
(D) Quantification of rRNA VAR1 and 45S pre-rRNA in wild-type *A. thaliana* root segments enriched in *H. schachtii*-induced syncytia by qPCR. Wild type plants were inoculated with *H. schachtii* J2s and root segments enriched in *H. schachtii*-induced syncytia (root+syncytium) and adjacent root segments without syncytia (root-syncytium; control) were dissected at 10 days post inoculation. In C and D, whole roots or

root segments cDNA was synthesized, and VAR1 and 45S pre-RNA were quantified by qPCR. *ACTIN 8* was amplified as reference.
In C and D, the experiments comprised three biological replicates, each consisting of three technical replicates. Similar results were obtained in the three independent experiments. Data of one representative experiment are shown.
For A, B, C and D, plants of the tested genotypes/treatments were grown in randomized block designs. For each biological replicate, plants were sampled randomly to prepare pools for each genotype/treatment.